Ethylene Receptor Gain- and Loss-of-function Mutants Reveal an ETR1-dependent Transcriptional Network in Roots

Running head: ETR1-dependent gene regulatory networks in roots

Maleana G. White[1*], Alexandria F. Harkey[1*], Joëlle K. Mühlemann[1,4], Amy L. Olex[2], Nathan J. Pfeffer[1], Maarten Houben[1,4], Brad M. Binder[3], Gloria K. Muday[1]

[1] Wake Forest University, Winston-Salem, NC

[2] Virginia Commonwealth University, Richmond, VA

[3]University of Tennessee, Knoxville, TN

[4]Current Address: KU Leuven, Belgium

*Co-first authors

One sentence summary: Transcriptional responses in *etr1* LOF and GOF mutants reveal an ethylene-mediated ETR1- and EIN3 dependent gene regulatory network that modulates ethylene signaling and synthesis and root development.

Abstract

In Arabidopsis, a family of five receptors mediates ethylene responses in roots, with Ethylene Response 1 (ETR1) controlling increases in root hair proliferation and decreases in lateral root formation. To define the ETR1-dependent gene regulatory network (GRN) controlling root development, we profiled the root transcriptome from Col-0 and the *etr1-3* gain-of-function and *etr1-7* loss-of-function mutants in the presence and absence of ethylene or the ethylene precursor 1-aminocyclopropane-1-carboxylic acid (ACC). We identified 4,522 differentially expressed (DE) transcripts in Col-0 roots with altered abundance in response to ethylene and/or ACC treatment, with larger magnitude changes induced by ethylene. These included 553 DE transcripts that were ETR1 dependent, defined by a lack of response to treatment with ethylene and/or ACC in ethylene-insensitive *etr1-3* and constitutively altered in *etr1-7* in the presence and absence of treatment relative to time-0 Col-0. Within these ETR1-dependent transcripts were ethylene biosynthesis genes and transcription factors. *ACC OXIDASE 2* (*ACO2)* and *ACO3* convert ACC to ethylene and were ETR1-dependent, and *ACO*-promoter-driven reporter fusions were ACC regulated in root tissues in appropriate locations to control root development, with *ACO5* localized to root hairs. Abundance of ETR1-dependent transcripts that were predicted to encode transcription factors and ACOs were examined in Col-0 and an *ein3eil1* mutant with and without ACC treatment, suggesting the ETR1 and EIN3/EIL1 canonical ethylene signaling pathway regulated some, but not all, of these transcriptional responses. Together, these findings reveal features of an ETR1-dependent GRN that controls both ethylene synthesis and root growth and development.

Introduction

Ethylene is a gaseous hormone that modulates growth and development throughout a plant's life cycle, from seed germination to senescence, and controls responses to both biotic and abiotic stress (Abeles et al., 1992; Van de Poel et al., 2015). In young, etiolated seedlings, ethylene induces a triple response: reduced hypocotyl and root elongation, thickening of the hypocotyl, and exaggeration of the apical hook. This triple response phenotype has been the basis of mutant screens in *Arabidopsis thaliana* that have identified key components of the ethylene signaling pathway with ethylene-insensitive or constitutive ethylene signaling phenotypes (Azhar et al., 2020; Schaller and Kieber, 2002). Ethylene also has profound effects on root development, including inhibition of primary root elongation and lateral root formation and stimulation of root hair initiation and elongation (Feng et al., 2017; Harkey et al., 2018; Lewis et al., 2011; Negi et al., 2008; Qin et al., 2019). Many of the proteins that were identified based on their functions in ethylene signaling in etiolated hypocotyls also modulate root development (Khoury et al., 2024b), but with distinct developmental effects downstream of each receptor (Harkey et al., 2018).

Ethylene functions through direct binding to members of a family of transmembrane receptors localized to the endoplasmic reticulum and the Golgi apparatus (Azhar et al., 2020; Binder, 2020; Schaller and Kieber, 2002). These receptors are negative regulators of the pathway, such that binding of ethylene to these receptors removes repression of the pathway, which initiates a signaling cascade that upregulates or downregulates genes with distinct transcriptional responses depending on the tissue type and growth conditions (Chang et al., 2013; Harkey et al., 2018, 2019; Stepanova et al., 2007). In Arabidopsis, five receptor isoforms have been identified: Ethylene Response 1 (ETR1), ETR2, Ethylene Insensitive 4 (EIN4), Ethylene

65 Response Sensor 1 (ERS1), and ERS2 (Binder, 2020; Chang et al., 1993; Hua et al., 1998; Hua
66 and Meyerowitz, 1998; Sakai et al., 1998; Schaller and Bleecker, 1995). Unlike most canonical
67 signaling pathways, ethylene receptors are active in the unbound state. In the absence of
68 ethylene, these receptors activate the Raf-like serine/threonine protein kinase Constitutive Triple
69 Response 1 (CTR1), destabilizing EIN3 and EIN3-like (EIL) transcription factors (TFs) and
70 blocking changes in gene expression downstream of these TFs (An et al., 2010; Binder, 2020;
71 Dolgikh et al., 2019; Kieber et al., 1993). In the bound state, however, the ethylene receptors
72 lead to stabilization of EIN3 and EIL TFs in an EIN2-dependent manner (Alonso et al., 1999; An
73 et al., 2010; Huang et al., 2003; Kieber et al., 1993; Qiao et al., 2009), leading to genome-wide
74 changes in transcript abundance (Chang et al., 2013; Harkey et al., 2018). Downstream of
75 EIN3/EIL are ethylene response factors (ERFs) and ethylene response DNA-binding factors
76 (EDFs) that further mediate transcription, consistent with the existence of tissue-specific gene
77 regulatory networks (GRNs) (Wang et al., 2002).

78 The function of ethylene signaling proteins in controlling root architecture has been
79 examined (Khoury et al., 2024b). EIN2 is required for root developmental responses to ethylene
80 and its immediate precursor 1-aminocyclopropane-1-carboxylic acid (ACC) at 1 μM (Alonso and
81 Stepanova, 2004; Negi et al., 2008), although a recent report indicates that treatment with ACC
82 at levels between 10 and 40 μM can alter root development in *ein2-5* (Mou et al., 2025). The
83 *ctr1-1* mutant was demonstrated to have constitutive-ethylene-signaling root phenotypes, with
84 this mutant having shorter primary roots and increased root hair proliferation compared to Col-0
85 seedlings in the absence of ethylene (Hua and Meyerowitz, 1998; Kieber et al., 1993; Masucci
86 and Schiefelbein, 1996; Rahman et al., 2000), suggesting its presence is required to suppress the
87 pathway in the absence of ethylene. EIN3 and EIL1 TFs function in ethylene-dependent root hair

88 formation, with the *ein3eil1* double mutant having reduced ACC-induction of root hair
89 proliferation (Feng et al., 2017). However, root developmental responses to ethylene can still be
90 observed in the *ein3* and *ein3eil1* mutants (Chang et al., 2013; Harkey et al., 2018), suggesting
91 that additional TFs may participate in these transcriptional responses to ethylene.

92 Recent studies have provided new insight into the mechanisms by which ACC is
93 converted to ethylene and identified conditions in which ACC affects plant development
94 independent of its conversion to ethylene. ACC is synthesized by the enzyme ACC synthase
95 from S-adenosyl methionine and then converted to ethylene via ACC oxidase (Houben and Van
96 de Poel, 2019). There are five ACC oxidase enzymes in Arabidopsis, and the transcripts
97 encoding these enzymes have been found to be regulated by ACC and ethylene, thereby
98 increasing ethylene levels in a feed-forward loop. Several quintuple mutants with defects in the
99 five *ACO* genes have now been used to demonstrate that ACC can affect root development in the
100 absence of ACO enzyme activity, providing evidence for actions of ACC independent of its
101 conversion to ethylene (Houben et al., 2024; Mou et al., 2025). The receptors that mediate the
102 regulation of ethylene synthesis by ACC and ethylene, and whether ACC might regulate ACO in
103 an ethylene-independent manner, have not been previously reported.

104 The five ethylene receptors in Arabidopsis each elicit distinct ethylene responses
105 (Shakeel et al., 2013), partially due to differences in receptor subunit structure and receptor
106 dimerization (Berleth et al., 2019). ETR1 was found to be the main receptor controlling
107 inhibition of ethylene perception by silver nitrate, nutational bending of hypocotyls, and
108 remodeling of root architecture (Harkey et al., 2018; McDaniel and Binder, 2012). In
109 Arabidopsis, ETR1 positively regulates nutational bending (Binder et al., 2006), while the other
110 four receptors negatively regulate this process (Kim et al., 2011). In roots, using a series of single

111 and multiple loss-of-function (LOF) and gain-of-function (GOF) mutants, only ETR1 was
112 needed for the inhibition of lateral root formation by ACC (Harkey et al., 2018). The inhibition
113 of lateral root formation by ACC was lost in the GOF, ethylene-insensitive mutant *etr1-3,* which
114 had significantly more lateral roots than wild type in the presence and absence of ACC. The
115 LOF, constitutive-signaling mutant *etr1-7* had significantly fewer lateral roots than wild type in
116 the presence and absence of ACC. ETR1 also has a central role in the inhibition of primary root
117 elongation and stimulation of root hair formation by ACC, consistent with ETR1 playing the
118 most substantial role in modulating ethylene-mediated root remodeling (Harkey et al., 2018).
119 Nevertheless, while it has been demonstrated that elevated levels of ethylene remodel the root
120 transcriptome (Harkey et al., 2018, 2019; Stepanova et al., 2007), the GRN downstream of the
121 ETR1 receptor has not yet been identified in roots.

122 To identify the ETR1-dependent GRN controlling ethylene- and ACC-regulated root
123 growth and development, we performed an RNA-Seq analysis in roots from light-grown
124 seedlings using Col-0 and ETR1 receptor GOF (*etr1-3*) and LOF (*etr1-7*) mutants. We identified
125 a core set of genes regulated by either or both ethylene and ACC in Col-0, including a subgroup
126 of these transcripts that we defined as ETR1-dependent due to mis-regulation in the mutants.
127 These transcripts had constitutively altered abundance in time-0 *etr1-7* (as compared to time-0
128 Col-0), and their responses to ACC and/or ethylene were lost in both *etr1-3* and *etr1-7* mutants.
129 We identified ACC- or ethylene-dependent regulation of transcripts encoding the ACOs, which
130 convert ACC to ethylene, revealing a subset that were ETR1-dependent. Analysis of verified
131 ACO transcriptional reporters driven by the native ACO promoters revealed overlapping and
132 distinct root tissue expression patterns among this protein family. Finally, we explored the
133 ETR1-dependent GRN through the lens of ETR1-dependent transcripts predicted to encode TFs,

134 building a network model that revealed TF-encoding transcripts with common temporal and
135 ETR1-regulated responses. We identified those TFs that are targets of EIN3 and tested whether
136 these transcriptional responses required functional copies of EIN3/EIL1. This work sheds light
137 on the ETR1 and EIN3-dependent GRNs that mediate the transcriptional responses to elevated
138 levels of ACC and its ethylene product.
139
140 **Results**
141
142 ***Ethylene and ACC doses with similar ETR1-dependent effects on root hair growth***
143 The main goal of this study was to define the genes that depend upon ETR1 for their
144 regulation by ethylene. We examined the transcriptional responses to both ethylene and its
145 immediate precursor ACC to compare their ETR1-dependent GRNs in these experiments, as
146 previous work suggested that ACC and ethylene may act through distinct signaling pathways in
147 some tissues (Houben et al., 2024; Mou et al., 2020; Yin et al., 2019). As a first step, we
148 determined the concentration of ethylene that yielded moderate root hair proliferation like that
149 induced by 0.75 µM ACC (Martin et al., 2022), by examining root hairs in Col-0 seedlings
150 treated with a range of ethylene levels for 24 hours (Supplemental Figure 1). The 0.3 ppm
151 ethylene concentration appeared to induce root hair proliferation to a similar degree as 0.75 µM
152 ACC, so we selected these concentrations for this RNA-Seq analysis. The effects of a 24-hour
153 treatment with these doses of ethylene and ACC were examined in the *etr1-3* and *etr1-7* mutants
154 revealing proliferation of root hairs in the *etr1-7* mutant in the absence of treatment (Figure 1B).
155 The ethylene-insensitive *etr1-3* mutant showed reduced responses to ACC and ethylene, forming
156 fewer and shorter root hairs in the presence of either treatment than Col-0. We used our

157 published ACC time-course microarray dataset (Harkey et al., 2018) to determine the time points
158 that had large numbers of differentially expressed (DE) genes that were not found in other time
159 points and overlapped with the early, middle, and late root hair developmental responses,
160 selecting 1, 4, and 24 hour treatment times (Supplemental Figure 2) (for details, see Methods).
161

162 ***The reduced effects of ACC and ethylene on transcriptional response in ETR1 mutants are***
163 ***revealed by principal component analysis***

164 We performed this RNA-Seq analysis in triplicate in root samples from three genotypes
165 (Col-0, *etr1-3*, and *etr1-7*), two treatments (0.75 µM ACC and 0.3 ppm ethylene gas), and four
166 time points (0, 1, 4, and 24 hours). After sequencing and quality control, principal component
167 analysis (PCA) plots were created using 1000 genes with the most variance between samples to
168 identify which factors contributed most to this variance. Figure 2A depicts the PCA plot for all
169 samples, which highlights differences between genotypes. The *etr1-7* samples (triangles) are
170 distinct with higher PC1 variance than Col-0 and *etr1-3*. There is a clear separation across PC2
171 between time-0 samples (in green) and ethylene- and ACC-treated samples (blue, purple, and
172 black symbols). Additionally, one time-0 Col-0 sample separated from other Col-0 time-0
173 samples along the PC2 axis, which prompted us to analyze variation *within* genotypes. These
174 plots (Supplemental Figure 3; described further in Methods) led us to remove the outlier Col-0
175 sample from downstream analyses.

176 We used three genotype-specific PCA plots (Figure 2B-D) to assess the contribution of
177 treatment type and duration to variation among samples within genotype. In Col-0 the time 0
178 samples (green circles) cluster together, consistent with the absence of exposure to ACC or
179 ethylene. The effect of treatment time is most evident in the separation between samples (circled

180 color groups) along the PC2 axes generally shifting from time 0 h to 24 h from the bottom to the
181 top of the axis. This PCA plot also emphasizes the difference between ethylene- and ACC-
182 treated samples across the PC1 axis, explaining 51% of the variance, suggesting unique
183 responses to these two molecules.

184 An important point that is revealed by these PCA plots is that both *etr1-3* and *etr1-7*
185 mutants have dampened response to treatment with ethylene and ACC, consistent with reduced
186 or enhanced signaling, respectively. In Col-0, PC1, which separates ACC and ethylene
187 treatments in all genotypes, explains 51% of the variance. In the mutants, PC1 explains only 35%
188 and 38% of the variance. Thus, the treatments have smaller effects on overall transcript
189 abundance changes in the mutants. This dampened response is also evident in *etr1-3* by the
190 overlapping responses of time 0 and 1 hour (green and blue samples) and the reduced separation
191 along PC2 for the 4- and 24-hour samples (purple and black), with especially tight clustering in
192 the 24-hour treatment. The *etr-7* samples show even less separation by time of treatment along
193 the PC2 axes (comparison of color of samples), especially for ACC-treated samples (open
194 circles), suggesting that this mutant is exhibiting ethylene and ACC responses in the absence of
195 treatment. Plots of Pearson's correlation (Supplemental Figure 4A and B) and of Euclidean
196 distance (Supplemental Figure 4C and D) with and without hierarchical clustering support these
197 conclusions, as do manually arranged plots grouped by genotype and time of ACC and ethylene
198 treatment (Supplemental Figure 4A and C; described further in Methods).

199

200 ***Ethylene treatment stimulated more dramatic transcriptional changes than ACC treatment in***
201 ***Col-0***

202 To summarize how the abundance of transcripts was affected by ethylene and ACC
203 treatment, we first examined the hormone-induced responses in Col-0. For both treatments, every
204 time point was compared back to the same set of combined Col-0 controls, defined above. We
205 created a density plot depicting the number of transcripts as a function of their $\log_2$FC using
206 those transcripts with a significant adjusted p-value < 0.01 as determined by DESeq2 (Figure
207 3A). We observed a bimodal distribution at each time point, showing one group of transcripts
208 that increased in abundance and another that decreased in abundance because of these treatments.
209 This pattern was found in response to both ethylene and ACC, although there were larger
210 numbers of DE transcripts and greater magnitude changes in response to ethylene than ACC
211 treatment, especially at one hour. Both treatments resulted in more down-regulated than up-
212 regulated genes at the 4- and 24-hour time points. The bimodal pattern and higher number of
213 down-regulated genes in response to ethylene and ACC at the 4- and 24-hour time points were
214 similar to our previous microarray study using ACC (Harkey et al., 2018). In all treatments and
215 time points, the bimodal peaks representing the increases and decreases in transcript abundance
216 relative to time-0 Col-0 were centered on or near -0.5 and 0.5 $\log_2$FC.

217 To identify genes with the most robust changes, we utilized a $|\log_2 FC| > 0.5$ and adjusted
218 p-value < 0.01 to define differential expression (DE) for the following analyses. Using DESeq2,
219 we identified 4,522 transcripts that were DE in response to ethylene and/or ACC in at least one
220 time point in Col-0 (Figure 3B-D). These transcripts and their $\log_2$FCs (treated Col-0 relative to
221 time-0 Col-0) are listed in Supplemental File 1. More transcripts responded to ethylene treatment
222 and had a greater $\log_2$FC than to ACC treatment. This $\log_2$FC cutoff eliminated more genes
223 whose transcripts decreased after treatment, which resulted in a similar number of up- and down-
224 regulated transcripts passing the $\log_2$FC cutoff, despite there being more down-regulated genes

225 in the larger set of those with a p-value < 0.01 (Figure 3A). Many genes showed similar trends in
226 response to ACC and ethylene treatment: 1,493 and 1,657 genes were down- and up-regulated,
227 respectively, by ethylene only, and 182 and 213 genes were down- and up-regulated,
228 respectively, by ACC only as summarized in Supplemental Table 2. Strikingly, only 16 genes
229 had opposite responses to the two treatments: three were down-regulated in ethylene and up-
230 regulated in ACC, and 13 were up-regulated in ethylene and down-regulated in ACC. This very
231 small number of oppositely regulated genes by these two treatments is consistent with ACC and
232 ethylene leading to common transcriptional responses, which may differ in magnitude of
233 response, but infrequently in the direction of responses.

234 This analysis also revealed that 457 and 504 transcripts were up- and down- regulated,
235 respectively, by both ACC and ethylene, with heatmaps illustrating the transcript abundance over
236 time in Figure 3C and D. One pattern that became apparent was that for transcripts whose
237 abundance decreased after both treatments, the 1- and 24-hour ACC-treated samples did not
238 respond as strongly as the time-matched ethylene-treated samples, while in the 4-hour ACC
239 treatment, the number of transcripts changed more dramatically than time-matched ethylene
240 treatment. This finding suggested the possibility that the rate of conversion of ACC to ethylene
241 resulted in varied ethylene concentrations across this time course. Indeed, of the 457 transcripts
242 up-regulated by both ACC and ethylene, 258 had a larger magnitude change in response to ACC
243 treatment at the 4-hour time point, but only 70% of them had a larger response to ethylene
244 treatment in the 1-hour time point. Similarly, of the 504 transcripts down-regulated by both ACC
245 and ethylene, 245 had a larger magnitude change in response to ACC treatment at the 4-hour
246 time point, with 87% of them responding more strongly to ethylene treatment at the 1-hour time
247 point. These results suggested that ACC induced maximal transcriptional responses more slowly

248 than ethylene, perhaps due to the time required to convert ACC to ethylene. Intriguingly, the
249 pattern of highest absolute $\log_2$FC at the 4-hour time point was also apparent in the transcripts
250 that were DE only in response to ACC treatment.
251
252 ***Transcripts regulated by ethylene and ACC were enriched in functions related to root***
253 ***development***
254 To determine which biological processes were enriched among the transcripts whose
255 abundance changed after ethylene and/or ACC treatment in Col-0, we performed Gene Ontology
256 (GO) analysis using AgriGO (Du et al., 2010; Tian et al., 2017) and reported the results in
257 Supplemental Table 3. Genes whose transcripts had increased abundance in both treatments were
258 enriched in functional annotations including "negative regulation of the ethylene-mediated
259 signaling pathway," which is consistent with both ethylene and ACC transcriptionally regulating
260 components of the ethylene signaling pathway in a negative feedback loop, and response to
261 auxin stimulus, consistent with crosstalk between ethylene and auxin.
262 Transcripts whose abundance decreased after ethylene and/or ACC treatment were
263 enriched in annotations pertaining to lignin biosynthesis and cell wall loosening, while
264 transcripts that decreased after ethylene but not ACC treatment were enriched in pathways
265 related to secondary cell wall biogenesis, plant-type cell wall organization, and lignin
266 metabolism. These results are consistent with the requirement for cell wall remodeling during
267 apical root growth, lateral root emergence, and root hair development.
268 Interestingly, genes whose transcripts decreased in abundance with ethylene treatment
269 only were enriched in annotations of root hair cell differentiation or root hair development,
270 including two myosin genes (*XIB* and *XIK*), *MORPHOGENESIS OF ROOT HAIR 1, 2*, and *6*,

271 *ROOT HAIR DEFECTIVE 4* (*RHD4*), *BRISTLED 1*, *CAN OF WORMS 1* (*COW1*), and *SHAVE 2*
272 and *3*. No annotations were significantly enriched in genes down-regulated by ACC only, likely
273 due to the smaller size of this group.

274 We further examined the identities of transcripts that were significantly regulated by
275 ACC but not by ethylene, as these transcripts might reveal ethylene-independent, ACC-mediated
276 signaling mechanisms in roots. Among the 213 transcripts that were uniquely up-regulated by
277 ACC were transcripts encoding two mitogen-activated protein (MAP) kinases MAPKKK13 and
278 MEK1, enzymes that remodel the cell wall, such as EXPANSIN A17 (EXPA17) and PECTIN
279 METHYLESTERASE 3 (PME3), and transcripts encoding proteins that function in root hair
280 development, such as RHO OF PLANTS GUANINE NUCLEOTIDE EXCHANGE FACTOR
281 12 (ROPGEF12) and ROOT HAIR DEFECTIVE 6-LIKE 5 (RSL5). Among the 182 transcripts
282 that were uniquely down-regulated by ACC were *EXPANSIN A4* (*EXPA4*) and *EXPANSIN-LIKE*
283 *A2* (*EXLA3*). These genes suggest testable hypotheses on mechanism for ACC-regulated root
284 development including cell wall remodeling, MAP kinase signaling, and membrane trafficking.
285

286 ***Transcriptional responses are accentuated in constitutive-signaling* etr1-7 *and reduced in***
287 ***ethylene-insensitive* etr1-3**

288 We asked how the transcriptional responses to ethylene and ACC varied in the *etr1-3* and
289 *etr1-7* mutants compared to Col-0. Using a cutoff of $|\log_2 FC| > 0.5$ and adjusted p-value < 0.01,
290 we compared each time point for each treatment and genotype to the Col-0 control and found
291 8,323 transcripts that were DE in at least one of these genotype comparisons, and these
292 transcripts and their $\log_2 FC$ values relative to time-0 Col-0 are listed in Supplemental File 1. A
293 heatmap displaying the changes in abundance of these transcripts in all three genotypes and both

294 treatments are shown in Figure 4. All $\log_2$FC values represented here were relative to Col-0 at
295 time 0 to accurately reflect the changes in baseline levels in *etr1-7*. The first striking observation
296 from this heat map is almost all the DE genes show the same directional change in response to
297 both ACC and ethylene, yet the magnitude of the response is larger in response to ethylene than
298 to ACC for most genes. Additionally, this heatmap hints at the muted response to treatment in
299 *etr1-3* and the enhanced transcript abundance independent of treatment in *etr1-7*.

300 The heatmap in Figure 4 suggested that the $\log_2$FC filter eliminated transcripts that
301 responded to ACC but had smaller magnitude changes in response to ACC than ethylene. As
302 illustrated in the density plots, many transcripts had a $|\log_2 FC|$ between 0.25 and 0.5, so we
303 examined transcriptional responses using a less stringent cutoff as detailed in the methods.
304 Regardless of cutoff, the number of transcripts that only responded to ethylene was greater than
305 those only responding to ACC, as shown in Supplemental Table 3, where the $|\log_2 FC| > 0.25$.
306 We therefore used the more stringent cut off in our experiments.

307 We compared baseline levels of expression in time-0 samples between genotypes (Figure
308 5A), identifying 2,562 genes that were DE (p-value < 0.01) in at least one of these comparisons
309 (these transcripts and their $\log_2$FC values relative to other genotypes are listed in Supplemental
310 File 1). Consistent with our expectations, *etr1-3* and Col-0 were nearly identical in the absence
311 of elevated ethylene; only 49 out of 2,562 genes were found to be DE between them. However,
312 when we compared *etr1-7* with either Col-0 or *etr1-3*, we found a dramatic difference: 1,941
313 genes were DE between *etr1-7* and Col-0, and 2,078 genes were DE between *etr1-7* and *etr1-3*.
314 A large number (1,458) of the genes were DE in both comparisons with *etr1-7,* including genes
315 enriched in the "response to ethylene" annotation (Figure 5B).

316 One very interesting group of transcripts were the 1,941 transcripts that were DE in *etr1-*
317 *7* as compared to Col-0, in the absence of hormone treatment. The large number and magnitude
318 change of these genes is consistent with the *etr1-7* mutation being sufficient to lead to large
319 changes in abundance of transcripts in the presence of endogenous levels of ethylene due to
320 enhanced ethylene signaling. Under these conditions, the *etr1-7* mutant has increased root hair
321 formation relative to Col-0. Consistent with this group of genes having an important function in
322 ethylene response, this group was enriched in annotations pertaining to the ethylene signaling
323 pathway. Similar annotations were also found in the group of transcripts that responded to
324 ethylene and/or ACC treatment in Col-0, including "response to ethylene" (Supplemental Table
325 3). These results are consistent with *etr1-7* having nearly constitutive ethylene signaling and
326 therefore a different transcriptional landscape than the other genotypes in the absence of
327 exogenous ethylene or ACC and with transcript abundance changes that overlap with Col-0 after
328 treatment with ACC or ethylene.
329
330 ***A subset of ACC- and ethylene-regulated transcript responses are dependent on ETR1***
331 We developed a rigorous set of criteria to determine which ethylene- and/or ACC-
332 regulated transcripts were dependent on ETR1 for transcriptional response. For this analysis, we
333 included transcripts that were DE in response to ACC or ethylene designated as a $|\log_2 FC| > 0.5$
334 and a p-value < 0.01 and defined transcripts as ETR1-dependent based on the following criteria:
335 1) the transcript was DE with ethylene and/or ACC treatment in at least one time point in Col-0;
336 2) the transcript showed no significant change in any *etr1-3* samples compared to Col-0 time 0;
337 and 3) the transcript was DE in *etr1-7* relative to Col-0 in the baseline and showed similar
338 abundance in ACC- and ethylene-treated *etr1-7* samples. Since *etr1-7* has constitutive ethylene

339 signaling, it should have had transcriptional responses that differed from Col-0 in the absence of
340 either ACC or ethylene treatment and were unchanged by ACC or ethylene treatment. Therefore,
341 we compared *etr1-7* treated samples to *etr1-7* control samples, and only those that did not change
342 with treatment in *etr1-7* qualified as ETR1-dependent.

343 With this strict criteria, 553 transcripts were identified as ETR1-dependent, which are
344 shown in the heat map in Figure 6 (and Supplemental File 1) with their $\log_2$FC values relative to
345 time-0 Col-0). A subset of 292 transcripts met these criteria in ethylene treatment only, another
346 191 in ACC only, and 70 genes were classified as ETR1-dependent in both treatments. The
347 patterns in this heat map are striking leading to four major conclusions. First, it is clear that the
348 *etr1-7* mutant leads to profound changes in transcript abundance (relative to time-0 Col-0) even
349 without treatment, which is evident in the time-0 *etr1-7* sample (labeled C), which is normalized
350 to the Col-0 time-0 sample) and that there are profound increases that are independent of
351 treatment. Second, there is a muted response in *etr1-3* that is evident for treatment with either
352 ethylene or ACC. Third, the response of these ETR1-dependent transcripts to ethylene is
353 generally greater than to ACC, which may be tied to potency of doses of these two molecules,
354 although ACC induced a larger effect at the 4-hour time point in Col-0, which is highlighted in a
355 green box on the heatmap. Fourth, the larger number of DE genes in response to ethylene than
356 ACC may be tied to a smaller magnitude of ACC response that was below the $\log_2$FC cutoffs,
357 suggesting that these transcripts are regulated by ETR1-dependent in both treatments. We also
358 examined the transcripts filtered to have a $|\log_2 FC| > 0.25$, which yielded many more transcripts
359 in each group, but did not change the overall ratios of transcripts in those groups.

360 Out of the 553 genes which qualified as ETR1-dependent in one or both treatments, 31
361 overlapped with a set of core ethylene-responsive genes identified by a comparison of three

362 transcriptome studies of ethylene- or ACC-treated roots (Harkey et al., 2019). These genes
363 included *ACC OXIDASE 2* (*ACO2*), *ETHYLENE RESPONSE SENSOR* (*ERS)1 & 2*, and
364 *ETHYLENE AND SALT INDUCIBLE 3* (*ESE3*). This finding suggested there were ETR1-
365 dependent transcriptional responses to ACC and ethylene in this core group. Other ethylene-
366 related genes that did not overlap with this group but were identified as ETR1-dependent here
367 included *ACO3*, several *ERFs*, and *PINOID*, a kinase that is a positive regulator of auxin
368 transport (Sukumar et al., 2009) and a negative regulator of root hairs (Lee and Cho, 2008). The
369 553 ETR1-dependent transcripts were enriched in GO annotations including lipid transport,
370 response to ABA, and regulation of transcription (Supplemental Table 4).

371 We tested an additional set of less stringent criteria, where response to treatment was
372 evaluated by comparing treated samples to the control samples within each genotype, but only
373 required presence or absence of treatment response regardless of the control sample abundance.
374 In this case, ETR1 dependence was defined by a response in Col-0 but not in the mutants, and
375 ETR1 independence was defined as a response in all three genotypes. This analysis allowed for a
376 larger set of transcripts to be included in both groups (Supplemental Figure 5), but ultimately the
377 changes in abundance of the additional transcripts were not as strong as those seen with the more
378 stringent criteria, so we focused our analysis on the transcripts that met the more stringent
379 criteria.

380

381 ***Other transcripts appear to be regulated by ACC and/or ethylene in an ETR1-independent or***
382 ***more complex manner***

383 We defined ETR1-independent responses for each treatment as having a response to
384 treatment in all genotypes and no altered response in the mutants at baseline (compared to time-0

385 Col-0). We compared the *etr1-7* treated samples to the *etr1-7* control samples to determine
386 whether a gene responded to treatment in this genotype relative to baseline transcript levels, but
387 in this case a response to treatment was required to qualify as ETR1-independent.

388 The search for ETR1-independent genes resulted in a slightly smaller set of genes: 481
389 genes qualified as ETR1-independent in ethylene only, 95 in ACC only, and 117 qualified in
390 both treatments (listed in Supplemental File 1 with their $\log_2$FC values relative to time-0 Col-0).
391 These ETR1-independent transcripts are shown in the heatmap in Figure 7, where the $\log_2$FC
392 relative to time-0 Col-0 was reported. What is very striking in this figure is the consistent pattern
393 of the genes that are DE in response to both ethylene and ACC show no difference in response in
394 all 3 genotypes. This trend is also true in the ethylene-only DE group, but the ACC response is
395 muted. The ACC only group had a very sporadic pattern with multiple different responses.
396 Another interesting observation was found among the ETR1-independent transcripts regulated by
397 both ACC and ethylene. Transcripts that were up-regulated by both treatments were rapidly
398 induced at the 1-hour time point, while transcripts that were down-regulated were more slowly
399 suppressed at the 4-hour time point. GO annotations enriched in this group of genes included
400 several stress-response annotations, as well as "root hair cell differentiation" and
401 "unidimensional cell growth" (Supplemental Table 4).

402 After grouping of genes into ETR1-dependent and -independent responses, there were an
403 additional 7,077 genes that were DE in response to ethylene- or ACC-treatment in at least one
404 sample but did not meet the criteria to fit in either group (listed in Supplemental File 1 with their
405 $\log_2$FC values relative to time-0 Col-0). These genes did not meet the strict criteria defined for
406 ETR1-dependent or -independent genes above, showing patterns of response inconsistent with
407 either definition (Supplemental Figure 6).

408

409 We also compared our ACC regulated genes to a recent dataset where *ein2-5* seedlings
410 were treated with 10 µM ACC for 40 hours to identify ACC-regulated transcripts (Mou et al.,
411 2025). This study identified 211 DE genes that were down-regulated and 147 that were up-
412 regulated by ACC. We asked whether these DE genes were also regulated by ACC in our root-
413 specific dataset, finding that, indeed, a majority of the up-regulated genes were (108 out of 147),
414 although only 17 out of 212 down-regulated genes were ACC regulated in our dataset, but over
415 100 of these were ethylene-regulated. We also asked if their DE genes were found in our ETR-
416 independent dataset, as the phenotypes of *etr1-3* and *ein2-5* mutants are similar. None of their
417 up-regulated genes were DE in response to ACC treatment in the ETR1-independent dataset,
418 while 32 of their up-regulated genes (22%) were ACC regulated in our ETR1-independent
419 dataset. The limited overlap between these two ACC-treatment datasets was unexpected, but
420 these differences could be due to seedling age, genotype, growth conditions, time of treatment,
421 and isolation of RNA from whole seedling versus roots.

422

423 ***Several ACOs are transcriptionally regulated by ACC and ethylene with some dependent on***
424 ***the ETR1 receptor***

425 An important action of both ACC and ethylene is to positively regulate the synthesis of
426 more ethylene. In particular, the ACC oxidase (ACO) enzyme catalyzes the oxidation of ACC to
427 ethylene as the final step of ethylene biosynthesis, which may use either endogenously
428 synthesized and exogenously applied ACC as a substrate. Included in the ETR1-dependent
429 dataset were transcripts encoding several of the five ACOs (*ACO1* through *ACO5*). The
430 transcript levels of *ACO1*, *ACO2*, and *ACO3* in each genotype and treatment are shown in Figure

431 8, revealing that transcripts encoding ACO enzymes are positively regulated by ACC and
432 ethylene levels, but with a stronger response to ACC. This ACC-driven increase in ACO enzyme
433 synthesis has the potential to increase conversion of exogenous ACC to ethylene. The abundance
434 of transcripts from these genes varied in time-0 Col-0 roots with higher transcript abundance of
435 *ACO2* and *ACO5* (313 and 315 TPM, respectively), while *ACO1*, *ACO3*, and *ACO4* had TPM
436 values between 6 and 39. We found that both ethylene and ACC treatment of Col-0 significantly
437 increased the transcript abundance of four *ACO*s (*ACO1*, *ACO2*, *ACO3*, and *ACO5*) in at least
438 one time point after treatment. For these genes, there was a greater magnitude increase in
439 transcript abundance in response to ACC than to ethylene treatment in at least one time point for
440 each transcript. This difference in response is striking as most of the up-regulated DE transcripts
441 in our dataset had larger magnitude changes in response to ethylene than to ACC treatment. This
442 finding suggests that exogenous ACC may be a stronger signal to promote transcript
443 accumulation of *ACO*s than ethylene gas itself.

444 According to our strict criteria for ETR1 dependence, detailed above, *ACO2* and *ACO3*
445 were ETR1-dependent in response to ethylene treatment, with uniform reductions in transcript
446 abundance in *etr1-3* and increases in *etr1-7* compared to Col-0 (Figure 8D, F). While *ACO2* and
447 *ACO3* passed the criteria for ETR1 dependence in Col-0 and *etr1-3* in response to ethylene
448 treatment, ACC induced significant increases in transcript abundance at one time point in the
449 *etr1-7* mutant relative to the *etr1-7* time-0 control and therefore these *ACOs* did not pass the
450 criteria for ETR1 dependence in the presence of ACC. *ACO1*, *ACO4,* and *ACO5* did not meet
451 our criteria for ETR1 dependence in the presence of either ACC or ethylene (Figure 8A, B;
452 Supplemental Figure 7). *ACO5* appeared to be ETR1-dependent based on p-value, but it failed
453 the $\log_2$FC cutoff for having a smaller magnitude change than required for our stringent

454 requirement. It is clear from the graphs that reduced or constitutive ethylene signaling in the
455 *etr1-3 and etr1-7* mutants, respectively, altered the transcriptional response to ACC and/or
456 ethylene for each *ACO*, consistent with the importance of the ETR1 receptor in regulating *ACO*
457 transcript abundance, even for *ACO*s that do not meet our stringent ETR1-dependent criteria.

458

459 ***ACC-induced transcript accumulation of ACO1, ACO2, and ACO4 is mediated by EIN3/EIL1***

460 To extend our understanding of the regulation of *ACO*s, we asked if their changes in
461 transcript abundance in roots were regulated by both ETR1- and EIN3-mediated GRNs. We
462 quantified the transcript abundance of the *ACO*s in roots of Col-0 and *ein3eil1* using RT-qPCR
463 in the presence and absence of 0.75 µM ACC. We treated these samples with ACC for 4 hours,
464 as this was the time point that yielded the largest increases in *ACO* transcript abundance (relative
465 to time-0 Col-0) in our RNA-Seq data. For *ACO1*, *ACO2*, and *ACO4*, we found significant
466 increases in transcript levels with ACC treatment in Col-0, including 2-fold increases in *ACO1*
467 and *ACO2* and a 1.5-fold increase in *ACO4* (Figure 8G-I). These ACC-induced increases were
468 lost in the *ein3eil1* mutant, consistent with these transcripts being ACC-regulated through the
469 canonical ethylene signaling pathway (Figure 8G-I). Consistent with our RT-qPCR results, the
470 promoters of *ACO2 and ACO4* were found to be directly bound by EIN3 in a DAP-Seq
471 (O'Malley et al., 2016) and/or ChIP-Seq dataset (Chang et al., 2013) as summarized in Harkey et
472 al. 2019, but the absence of *ACO1* as an EIN3 target is surprising and is consistent with an EIN3-
473 regulated TF binding to and controlling *ACO1* transcription, rather than being a direct EIN3
474 target.

475 In contrast, we did not detect significant increases in *ACO3* and *ACO5* transcripts in
476 response to ACC treatment in Col-0 in our RT-qPCR (Supplemental Figure 8). *ACO3* transcript
477 levels in *ein3eil1* did not differ from those in Col-0 in the presence or absence of ACC, while
478 *ACO5* transcript levels in Col-0 ACC-treated samples were significantly higher than those in
479 *ein3eil1* in the presence and absence of ACC (Supplemental Figure 8). For both *ACOs*, these
480 findings were consistent with localized changes in abundance in specific tissues that cannot be
481 consistently detected by RT-qPCR using whole roots.

482

483 ***ACO transcription increases in distinct root cell types in response to ACC treatment***

484 To determine which of the *ACO*s might control ACC- and ethylene-induced changes in
485 root development, we queried the *ACO*s in a root cell-type-specific dataset (Brady et al., 2007) to
486 identify the tissues where these transcripts were most highly enriched. We searched for
487 transcripts that were localized in the appropriate tissues to mediate ACC- and ethylene-induced
488 root responses, including stimulation of root hair initiation, inhibition of lateral root emergence
489 and inhibition of root elongation at the root tip. *ACO5* was identified as a candidate for the
490 control of root hair growth because, like *ETR1*, its transcripts were highly enriched in cells
491 expressing root hair markers, while the other *ACOs* had low transcript abundance in this cell type
492 (Figure 9A).

493 To provide additional insight into the effect of ACC treatment on tissue-specific
494 localization and abundance of *ACO* transcripts, we examined a fluorescent reporter driven by
495 each of the native *ACO* promoters (Houben et al., 2024). To validate the root hair cell specific
496 *ACO5* accumulation in the microarray described above, we examined fluorescence of a

497 *pACO5*::GFP-GUS reporter in roots. Comparison of root tip with and without a 4 hour ACC
498 treatment reveals low levels of GFP signal at the root tip with higher levels in the elongation and
499 differentiation zones. The GFP signal is evident in hair cells and root hairs, which are increased
500 in number after ACC treatment (Figure 9B). Laser scanning confocal microscope (LSCM)
501 images of root tips of 5-day-old seedlings revealed brighter fluorescence in hair cells than non-
502 hair cells, consistent with cell-type-specific expression patterns (Figure 9B; Figure 10).
503 Treatment with ACC for 4 and 24 hours (Figure 9C) or 5 days (Supplemental Figure 9) led to
504 increased number and elongation of root hairs, further illustrating the presence of *pACO5* driving
505 GFP fluorescence in these cells (Figure 9B). These results indicate that *ACO5* is expressed in the
506 appropriate position for its protein product to synthesize ethylene to drive root hair elongation.

507 We found shared and distinct ACO expression patterns in roots of 10-day-old seedlings
508 in the presence and absence of 0.75 μM ACC after five days of treatment (Figure 10). The
509 *pACO1*::GFP-GUS reporter had a fluorescent signal in the lateral root cap and the columella of
510 primary and lateral root tips, where this signal was increased in response to ACC treatment. The
511 *pACO3*::GFP-GUS reporter exhibited a fluorescent signal in the primary root columella and the
512 inner tissues of primary and lateral roots, where this signal was increased in response to ACC
513 treatment. Interestingly, the *pACO4*::GFP-GUS reporter had a fluorescent signal in the columella
514 of elongated lateral roots that was increased after ACC treatment, but this signal was not detected
515 in the columella of primary root tips in the presence or absence of ACC. We identified weak
516 ACC-induced changes for some of the reporters in the root tissues of interest, although there
517 appeared to be moderate basal levels of expression consistent with the cell type data (Figure 10).
518 The fluorescence of the *pACO2*::GFP-GUS reporter was low and did not show induction by
519 ACC in root tissues of interest (Supplemental Figure 10). These diverse expression patterns of

520 the *ACO* reporters suggest that the conversion of ACC to ethylene may be controlled at the tissue
521 level locally elevate ethylene signaling.

522

523 ***Identification of EIN3-regulated transcripts predicted to encode TFs within the ETR1-***
524 ***dependent GRN***

525 One goal of this study was to gain additional insight into the transcriptional regulators
526 downstream of ETR1 whose abundance changed in response to ACC and ethylene treatment.
527 Consistent with a global remodeling of the transcriptome, a GO analysis revealed that the ETR1-
528 dependent transcripts were significantly enriched in genes that function in the regulation of
529 transcription (Supplemental Table 4). We identified 60 ETR1-dependent transcripts predicted to
530 encode TFs using the AGRIS database (Palaniswamy et al., 2006). The expression patterns of
531 these TF-encoding transcripts were calculated and the $\log_2$FC relative to time-0 Col-0 is shown
532 in Figure 11A. Note the larger number of down-regulated than up-regulated transcripts and the
533 distinct temporal responses, with some transcripts changing rapidly after ACC and/or ethylene
534 treatment and other transcripts responding more slowly to these treatments.

535 To better visualize groups of TFs that have similar expression patterns in response to
536 treatments and in the *etr1* mutants, we employed a PaLD analysis (Berenhaut et al., 2022;
537 Khoury et al., 2024a) using the $\log_2$FC values relative to Col-0 time 0 for each transcript to
538 generate a network of the 60 ETR1-dependent TFs (Figure 11B). This analysis results in a
539 network with each node representing one of the 60 TF-encoding transcripts and the edges
540 connecting transcripts with the most similar responses to ACC and ethylene over time in the
541 different genotypes.

542 To sort these transcripts into distinct groups with the most similar responses, we used the
543 Louvain method, which identifies communities in large networks (Blondel et al., 2008). The
544 network yielded a structure consisting of six groups containing two or more transcripts.
545 Transcripts belonging to the same group as indicated by their matching colors are those with the
546 most similar transcript abundance patterns across the time course of ACC and ethylene treatment
547 in Col-0, *etr1-3*, and *etr1-7*. As EIN3 is a transcription factor that is downstream of ETR1 in the
548 canonical ethylene signaling pathway (Dolgikh et al., 2019), we used publicly available data on
549 the genes to which EIN3 binds revealed by DAP-Seq (O'Malley et al., 2016) or ChIP-Seq
550 (Chang et al., 2013). We highlighted on the PaLD network in large, bold font the direct targets of
551 EIN3. Consistent with EIN3 functioning to primarily increase transcript abundance, most of the
552 targets were found in the up-regulated groups of genes (Figure 11B). We also calculated the
553 percent of genes in each Louvain group that are direct EIN3 targets. The pink and yellow groups
554 making up the up-regulated transcripts consisted of 71% and 31% EIN3 targets, respectively.
555 These numbers are substantially higher than the 4% of the whole genome containing EIN3
556 targets. In contrast, the green, blue, orange, and red-orange groups consisting of down-regulated
557 transcripts included 25%, 8%, 0%, and 0% EIN3 targets, respectively. The up-regulatedEIN3
558 targets had diverse expression patterns, with some being rapidly induced (e.g., *ERF2*) or
559 repressed (e.g. AT1G08320) by ACC/ethylene treatment, and others being more slowly up-
560 (e.g., *RSL5*) or down-regulated (e.g. *MYB9* and *MYB107*).

561 To validate whether both up-regulated and down-regulated ETR1-dependent transcripts
562 that are EIN3 targets by ChIP-Seq and DAP-Seq showed altered transcript abundance in the
563 *ein3eil1* mutant, we quantified the transcript abundance of several genes in roots of five-day-old
564 Col-0 and *ein3eil1* seedlings in the presence and absence of ACC after 4 hours. We were

565 interested in *ROOT HAIR DEFECTIVE 6-LIKE 5* (*RSL5*), as this TF was previously
566 demonstrated to be involved in root hair development (Pires et al., 2013). Intriguingly, in our
567 RNA-Seq dataset, *RSL5* transcript levels were significantly up-regulated by ACC at the 4- and
568 24-hour time points but were not significantly regulated by ethylene (Figure 11C, D). Consistent
569 with these data, we found a significant increase in *RSL5* transcripts in the presence of ACC and
570 demonstrated the dependence of this change on EIN3, as this induction was lost in the *ein3eil1*
571 mutant (Figure 11E). This result suggested that although *RSL5* was more strongly regulated by
572 ACC, this regulation depended upon the canonical ethylene signaling pathway. We also observed
573 a significant increase in *RAP2.6L* transcript levels and a significant decrease in *MYB9* transcript
574 levels in the presence of ACC, and both changes were lost in the *ein3eil1* mutant (Figure 11F,
575 G). We also examined transcript abundance of an additional gene (*LRP1*) whose promoter was
576 targeted by EIN3, and three genes (*ANAC058*, *MYB52*, and *MYB93*) that were not identified as
577 direct targets of EIN3 by ChIP-Seq and DAP-Seq (Chang et al., 2013; O'Malley et al., 2016).
578 However, the levels of these transcripts were not significantly altered by ACC in our RT-qPCR
579 data, although there were trends consistent with the patterns observed in the RNA-Seq data
580 (Supplemental Figure 11). This example further validates the ability of this RNA-Seq dataset to
581 identify additional root-specific genes that are dependent upon ETR1 and EIN3 for altered
582 transcript accumulation in response to ACC and/or ethylene treatment.

583 ***The proLRP1::GUS reporter exhibited increased amounts of GUS product in lateral root***
584 ***primordia in the presence of ACC***

585 We were interested in exploring the roles of several of these ETR1-dependent TFs in root
586 development and how they were modulated by ACC. We examined *LRP1* since it had previously
587 been demonstrated to function in lateral root primordium (LRP) development, as *LRP1*

588 overexpression lines had increased numbers of stage I, IV, and V LRP, but reduced numbers of
589 emerged lateral roots (Singh et al., 2020). Since *LRP1* transcripts were induced in whole roots in
590 response to ethylene and ACC treatment (Figure 12A, B), we next asked in which root tissues
591 these transcripts were synthesized. We used the *proLRP1*::GUS transcriptional reporter
592 (Estornell et al., 2018) treated with ACC for five days and visualized GUS product in roots using
593 a stereomicroscope. In 10-day-old seedlings, we found the GUS product accumulated in the
594 central root tissues in both the presence and absence of ACC, beginning at the root elongation
595 zone (Figure 12C). We observed increased GUS activity in the presence of ACC in lateral root
596 primordia at all primordia stages and in emerged lateral roots, with darkest staining evident in the
597 stele layers, consistent with *LRP1* transcripts being synthesized in these tissues and having
598 increased expression in response to ACC treatment.

599 We also quantified the number of lateral roots and the lateral root density in the region of
600 new root growth in the *lrp1-1* and *lrp1-2* mutants in the presence and absence of ACC, with
601 representative images shown in Supplemental Figure 12A. Based on a prior report that examined
602 *LRP1* overexpression lines and identified a 2.5-fold decrease in lateral root density in these lines
603 compared to Col-0 (Singh et al., 2020), we expected an increase in lateral roots in *lrp* mutants.
604 We quantified the number of lateral roots in the region of root formed after transfer to control or
605 ACC media, as we previously demonstrated a negative effect of ACC on lateral root formation in
606 this region (Negi et al., 2008). We found that in time-0 roots, there was a small and significant
607 increase in the number of emerged lateral roots in *lrp1-1* with a non-significant increase in *lrp1-2*
608 (Figure 12E). We found that these small differences were lost in the presence of ACC, which had
609 equivalent inhibition of lateral root formation as Col-0. We also quantified lateral root density in
610 the region of new root growth (5 days of ACC treatment) and found no significant difference in

611 lateral root density in *lrp1-1* and *lrp1-2* in the absence of ACC (Supplemental Figure 12B). The
612 reduction in lateral root density by ACC significantly differed from Col-0 in *lrp1-2* and not *lrp1-*
613 *1*, with less inhibition of lateral root formation in *lrp1-2* compared to Col-0. Consistent with the
614 weak accumulation and the absence of changes with ACC of the *proLRP1*::GUS reporter in the
615 primary root tip (Figure 12C), there were subtle changes in primary root elongation in the
616 mutants (Figure 12D). We observed a small but statistically significant increase in primary root
617 growth in *lrp1-1* in the absence of ACC and no significant increase in *lrp1-2* compared to Col-0.

618

619 ***Several ETR1-dependent TF mutants show subtle differences in root hair initiation, lateral***
620 ***root formation, and root elongation***

621 We screened mutants in a small set of ETR1-dependent TFs for root phenotypes in the
622 presence and absence of ACC. We selected several genes that were also regulated by ACC over
623 a time course of ACC treatment (Harkey et al., 2018). These included *RAP2.6-L*, *ANA058*,
624 *MYB9*, and *MYB52*, some of which were also found to be direct targets of EIN3. To illustrate
625 how these genes responded to ethylene and ACC treatment in Col-0, *etr1-3*, and *etr1-7* in this
626 RNA-Seq study, we reported the fold change in transcript abundance relative to time-0 Col-0
627 (Supplemental Figure 13). These transcripts were also expressed in various root tissues,
628 including lateral roots, pericycle cells, xylem pole pericycle cells, hair cells, and non-hair cells to
629 varying degrees (Supplemental Figure 14A).

630 We found that in the region of new root growth, *myb52-1* had significantly fewer lateral
631 roots than Col-0 in the absence of ACC, but it showed wild-type inhibition of lateral root
632 formation in the presence of ACC (Supplemental Figure 14B). The *anac058-1*, *myb52-1*, and

633 *rap2.6l-1* mutants all had lower lateral root densities in this region in the presence of ACC
634 compared to Col-0, suggesting they may function to promote lateral root formation
635 (Supplemental Figure 14C). These results were consistent with *MYB52* and *ANAC058* being
636 down-regulated by ACC, but not with *RAP2.6L* being up-regulated by ACC. The *myb9-1* mutant
637 was also found to have a longer primary root growth phenotype in the absence of ACC compared
638 to Col-0, and no difference was observed in the presence of ACC (Supplemental Figure 14D),
639 suggesting MYB9 may inhibit primary root growth, although this was not consistent with MYB9
640 being down-regulated by ACC. We also examined the effects of these mutants on root hair
641 number in the absence and presence of four hours of ACC treatment. Only the *myb52-1* mutant
642 had aberrant root hair formation with reduced root hairs compared to Col-0 in both the presence
643 and absence of ACC, suggesting it functions to promote root hair formation (Supplemental
644 Figure 15). These subtle phenotypes were likely due to functional redundancy, as many of the
645 proteins encoded by these transcripts belonged to extensive TF families.

646 We also compared the growth response of the light-grown seedlings described above to
647 dark-grown seedlings (Supplemental Figure 16). In 10-day-old light-grown seedlings, the *lrp1-1*
648 and *myb9-1* mutants exhibited more primary root growth, yet the ability of ACC to inhibit
649 elongation was like that observed in Col-0, with other mutants having Col-0 levels of root
650 elongation in the absence of treatment (Supplemental Figure 12B; Supplemental Figure 14B).
651 When these same mutants were etiolated on ACC (or untreated) plates for four days, we found
652 that *lrp1-1* had significantly shorter roots than Col-0 at 0.2 μM ACC, while *myb9-1* behaved like
653 Col-0 at all doses of ACC we tested. We also found that *rap2.6l-1*, which did not have a primary
654 root growth phenotype when grown under continuous light, displayed shorter roots than Col-0 at
655 multiple lower doses of ACC (<0.5 μM) after etiolation. However, *lrp1-1* and *rap2.6l-1* did not

656 differ from Col-0 at ACC doses of 0.5 µM and higher. The *myb52-1* mutant displayed longer
657 roots than Col-0 under control conditions at five days of age, although the primary root growth
658 did not differ from Col-0 at 10 days of age when lateral roots were measured. In contrast,
659 etiolated *myb52-1* seedlings displayed longer roots than Col-0 in the absence of ACC treatment
660 but shorter roots than Col-0 in the presence of 0.2 µM ACC. The *anac058-1* mutant was not
661 significantly different from Col-0 at any of the doses of ACC we tested. These differences in
662 light- and dark-grown seedlings suggested that perhaps some of the ETR1-dependent TFs were
663 more important for light-dependent root responses than light-independent ones (Harkey et al.,
664 2019).

665

666 **Discussion**

667 The Arabidopsis genome encodes five ethylene receptors that have distinct and
668 overlapping functions in the regulation of plant growth. These receptors negatively regulate the
669 ethylene signaling pathway and are turned off by ethylene binding, inducing downstream
670 changes in transcription. The specific roles of individual receptors in controlling ethylene-
671 regulated development have been examined only in a few tissues (Binder, 2020; Cancel and
672 Larsen, 2002; Harkey et al., 2018; Ma and Dong, 2021). In roots, ETR1 is the ethylene receptor
673 that is most strongly linked to the inhibition of both lateral root formation and primary root
674 elongation and the stimulation of root hair growth (Harkey et al., 2018). To identify the
675 transcripts whose synthesis is regulated by ETR1 to control root development, we identified
676 genome-wide changes in transcript abundance in roots in response to treatment with ethylene or
677 its precursor, ACC, using Col-0 and LOF and GOF *etr1* receptor mutants. We examined the

678 GRNs that are turned on by ethylene and ACC and are dependent on ETR1 signaling, revealing
679 transcripts encoding enzymes of ethylene synthesis and TFs that have the potential to drive
680 transcriptional responses downstream of ethylene.

681 To identify the transcriptional changes in the presence and absence of ethylene and ACC
682 in Col-0, we treated seedlings with ethylene or ACC and the transcript abundance in roots were
683 quantified at several time points after treatment (0, 1, 4, and 24 hours), and transcript abundance
684 relative to time-0 Col-0 was used to identify DE transcripts and the direction and magnitude
685 change of abundance of these transcripts. Ethylene induced a greater number of DE genes than
686 ACC at all time points after treatment, and the magnitude change of these DE genes was larger
687 (Figure 3). The most likely explanation for this result was that ethylene gas used in our
688 treatments elevated ethylene levels more than this dose of ACC. The majority of changes in
689 transcript abundance in response to either ethylene or ACC treatment were decreases in
690 abundance, especially at the 4- and 24-hour time points. This observation is in alignment with
691 other reports that ACC treatment led to a greater number of transcripts with decreased abundance
692 than increased abundance relative to time-0 controls in Col-0 and in the ethylene-insensitive
693 *ein2-5* mutant (Harkey et al., 2018; Mou et al., 2025).

694 Several reports have suggested that ACC may act as a signal independently of its
695 conversion to ethylene, especially at high concentrations where ACO-dependent conversion of
696 ACC to ethylene becomes rate limiting (Althiab-Almasaud et al., 2021; Houben and Van de
697 Poel, 2019; Li et al., 2020, 2022; Mou et al., 2020, 2025; Polko and Kieber, 2019; Tsang et al.,
698 2011; Tsuchisaka et al., 2009; Van de Poel, 2020; Van de Poel and Van Der Straeten, 2014;
699 Vanderstraeten et al., 2019; Xu et al., 2008; Yin et al., 2019). At concentrations of 10 μM and
700 above, ACC inhibits rosette size and growth across all tissues in seedlings (Vanderstraeten et al.,

701 2019) and stimulates lateral root initiation and emergence (Mou et al. 2025). However, in roots at
702 lower doses of ACC (less than or equal to 1 μM), both the ethylene-insensitive *ein2-1* and *ein2-5*
703 mutants do not respond to treatment with 1 μM ACC (Harkey et al., 2018; Ivanchenko et al.,
704 2008; Muday et al., 2012; Negi et al., 2008; Růžička et al., 2007), suggesting that ACC is either
705 largely converted to ethylene at this dose or that in these tissues under these growth conditions
706 ACC predominantly acts via its conversion to ethylene. Our finding that most of the transcripts
707 that were DE in response to this low dose of ACC were also DE in response to ethylene is
708 consistent with these possibilities. Yet the presence of transcripts in this dataset whose
709 abundance changed after regulated by ACC-treatment, but not ethylene-treatment, even though
710 ethylene generally resulted in more robust transcript abundance changes, is consistent with ACC
711 having a direct effect on transcription.

712 A recent article described a mechanism by which ACC-regulated transcripts may result
713 from direct ACC signaling to TFs rather than signaling after its conversion to ethylene. ACC has
714 been shown to regulate WOX5 and LBD18 to control meristem growth and lateral root
715 development, respectively, independent of ethylene signaling (Mou et al., 2025). The majority of
716 the positively ACC-regulated DE transcripts identified in their udataset when ethylene-
717 insensitive *ein2-5* seedlings were treated with ACC were also DE in response to ACC in our
718 dataset, although not the downregulated genes, consistent with conserved transcriptional
719 responses between our datasets.

720 We found that several transcripts regulated by only ACC included those encoding MAP
721 kinases, enzymes that remodel the cell wall, and proteins involved in root hair development, as
722 well as ACO enzymes whose regulation we characterized. We found that ACC down-regulated

723 *ACS7*, which might suggest a negative feedback of ACC synthesis in response to elevated levels
724 of ACC, while *ACO* transcripts increase to facilitate conversion to ethylene.

725 An important goal of these experiments was to take the large number (8,323) of DE genes
726 in response to ethylene and/or ACC (Figure 4) and refine this dataset by identifying the genes
727 whose regulation of depended on ETR1. We identified ETR1-regulated genes using two *etr1*
728 mutant alleles: *etr1-3*, which is a GOF receptor mutant with a constitutively active receptor that
729 turns off ethylene signaling, resulting in an ethylene-insensitive phenotype, and *etr1-7*, which is
730 a LOF receptor mutant that has an inactive receptor, resulting in constitutive ethylene signaling.
731 The combination of GOF and LOF receptor mutants served as a powerful approach to identify
732 ETR1-dependent transcriptional responses. This is clear from the earliest steps of the analysis;
733 comparison of all samples by a PCA plot, Pearson's correlation, and Euclidean distance plots led
734 to the separation of *etr1-7* samples from Col-0 and *etr1-3* on the PC1 axis (Figure 2A).

735 We used a strict criterion to define the ETR1-dependent genes, requiring genes were DE
736 with either ethylene or ACC, significantly altered in abundance in the *etr1-7* allele, with
737 constitutive ethylene response, and transcripts were not significantly changed by ethylene or
738 ACC in the ethylene insensitive *etr1-3* mutant. The pattern of response evident in Figure 6 shows
739 enhanced transcript abundance in *etr1-7* that is not changed by either ethylene or ACC treatment,
740 with these transcripts having muted response to both hormones. The strict ETR1-dependent
741 group was enriched in transcripts annotated to function in "ethylene mediated signaling
742 pathway." We also compared our ETR1 dependent genes to a conserved group of ethylene-
743 responsive genes from a meta-analysis of three root ACC and ethylene response datasets (Harkey
744 et al. 2019) finding 31 transcripts that were ETR dependent in the overlap of these groups.

745 An unexpected finding in this study was that there were nearly as many transcripts that
746 responded in an ETR1-independent fashion as those that were ETR1-dependent (Figure 7).
747 Transcripts were defined as ETR1-independent if they responded to ACC or ethylene treatment
748 in all three genotypes. If the abundance of these transcripts increased and decreased in *etr1-7* and
749 *etr1-3*, respectively, and changed with hormone treatment, this might suggest two receptors
750 control their activity, with hormone-dependent changes being mediated by a second receptor. In
751 a prior study we found ETR1 to be essential in some root developmental responses and identified
752 roles for other ethylene receptors in other responses (Harkey et al., 2018). ACC effects on lateral
753 root development were completely lost in the ethylene-insensitive mutant *etr1-3* and not induced
754 by addition of ACC in the constitutively signaling mutant *etr1-7*, suggesting inhibition of lateral
755 root formation by ethylene signaling had strong dependence on ETR1. In contrast, inhibition of
756 primary root elongation and stimulation of root hair growth by ACC were less dependent on
757 ETR1 as they showed attenuated responses to ACC in *etr1-7* (Harkey et al., 2018), suggesting a
758 role of other ethylene receptors in these root processes. Perhaps some of the transcripts which
759 were ETR1 independent were involved in root elongation or root hair initiation. Indeed, when we
760 examined genes that were ETR1-independent by the strictest criteria, they were enriched in the
761 annotation "root hair cell differentiation" and several other related annotations.

762 We had identified a small subset of transcripts that were regulated only by ACC in Col-0,
763 suggesting responses that may be driven by ACC signaling independently of its conversion to
764 ethylene. Therefore, we were interested in further analyzing the transcripts that encode ACC
765 oxidases, which convert ACC to ethylene, as this might provide insight into understanding how
766 ACC may regulate its conversion to ethylene.

767 In our dataset, we found that *ACO* transcripts were themselves regulated by ACC and
768 ethylene in a positive feed forward loop, where application of ethylene and/or ACC induced
769 transcript accumulation of all *ACO*s in at least one time point after treatment (Figure 8). We
770 found that *ACO2* and *ACO3* met our strict criteria for ETR1 dependence in response to ethylene
771 but not ACC. This suggests that ACC may be able to regulate transcripts in ways above and
772 beyond the function of ETR1, consistent with the possibility of an ACC-independent signaling
773 pathway. However, for *ACO2*, perhaps the most puzzling of the *ACO*s, ACC-mediated changes
774 in transcript abundance were completely lost in *ein3eil1*, suggesting that ACC activates the
775 canonical ethylene signaling pathway to control *ACO2* levels. It is not clear how ACC both
776 activates the canonical ethylene signaling pathway and induces changes in the *etr1* mutants that
777 were not induced by ethylene. Perhaps ACC can work through a non-canonical ethylene
778 signaling pathway or directly bind to a different ethylene receptor, as this might be required
779 when ACC levels become too high, and the plant needs a mechanism to rapidly convert ACC to
780 ethylene. There is evidence that glucose can signal to EIN2 and subsequently EIN3/EIL1 through
781 the target of rapamycin pathway (Fu et al., 2021), so it is possible that ACC could activate this or
782 a similar pathway resulting in transcriptional changes that are not dependent on ETR1 but require
783 the EIN3/EIL1 machinery.

784 To provide more information on the localization of changes in *ACO* transcript abundance,
785 we examined the root cell-type-specific localization of *ACO* transcripts in untreated roots using
786 publicly available transcriptome data and *in planta* using ACO promoter-driven fluorescent
787 protein reporters to inform our understanding of the tissues that express the machinery to convert
788 ACC to ethylene under our treatment conditions (Figures 9 and 10). We found that each *ACO*
789 had a distinct tissue expression pattern, and many of these were enhanced in the presence of

790 ACC treatment in 10-day-old seedlings. These findings were consistent with *ACO*s being
791 expressed in root hairs, lateral roots, pericycle cells, and the root elongation zone where their
792 protein products convert ACC to ethylene to signal root responses in these tissues. The most
793 striking observation was that *ACO5* transcripts were the only *ACO* accumulating to high levels in
794 hair cells prior to and after root hairs initiated, and this root hair expression was evident in ACC-
795 treated seedlings that formed more and longer root hairs, consistent with a role for ACO5 in
796 driving root hair elongation. The other *pACO*::GFP reporters were not detected or had low
797 fluorescence in root hairs.

798 We were interested in mapping the GRN downstream of ETR1 and EIN3/EIL1 by
799 examining transcripts predicted to encode TFs using the Agris database (Davuluri et al., 2003).
800 We identified 60 TF-encoding transcripts in the ETR1-dependent list of genes and found some
801 that were rapidly up-regulated and a greater number that were down-regulated by ACC and
802 ethylene treatment with a range of different kinetic responses to these treatments (Figure 11). We
803 also generated a network using PaLD, which groups transcripts together with the most similar
804 temporal responses. This network allows us to visualize connections among transcripts with the
805 most similar responses to ACC and ethylene across time and genotypes and to partition
806 transcripts into groups of like responding genes. We found that the up-regulated genes clustered
807 into two groups, one consisting of transcripts with rapid and strong induction in response to
808 treatment, and another consisting of transcripts with more muted up-regulatory patterns, and both
809 groups were enriched in direct targets of EIN3. In contrast, the down-regulated genes clustered
810 into four groups containing two or more transcripts with distinct expression patterns, and few of
811 the transcripts in these groups were direct targets of EIN3. These results raise the interesting

812 question of what is the regulatory mechanism by which so many of these transcripts have
813 decreased abundance in response to ACC and ethylene treatment.

814 We asked whether three of the TF-encoding genes that were found to be EIN3 targets in
815 DAP-Seq or ChIP-Seq datasets (Chang et al. 2013; O'Malley et al. 2016) lost their ACC-
816 regulated expression in an *ein3eil1* mutant, focusing on *ROOT HAIR DEFECTIVE 6-LIKE 5*
817 (*RSL5*), *RELATED TO AP2 6L (RAP2.L)*, and *MYB9* (Figure 11). We found that the ACC-
818 mediated increase in *RSL5* and *RAP2.6L* transcripts and the decrease in *MYB9* transcripts were
819 both lost in *ein3eil1*. It was previously reported that an *rsl5* mutant exhibited normal root hair
820 development in the absence of treatment (Pires et al. 2013), which is not surprising due to the
821 low levels of transcript abundance (2 TPM) in time-0 roots, suggesting that RSL5 might function
822 in ACC- and ethylene-stimulated root hair formation. An interesting question that arises from
823 this work is how ETR1 regulates genes that are not regulated by EIN3/EIL1. It is possible that
824 ETR1-dependent genes could be regulated by the non-canonical AHP and ARR families (Binder
825 et al. 2020), as previous work demonstrated direct interaction and phosphorylation between
826 ETR1 and AHP1 in vitro (Scharein and Groth, 2011).

827 ETR1 is important in ethylene's ability to inhibit lateral root formation in the region of
828 new root growth formed after exposure to ACC. *LRP1* was identified as ETR-dependent in our
829 dataset; this gene encodes a TF that has previously been shown to function in inhibiting lateral
830 root emergence downstream of ARF7/ARF19, LATERAL ROOT PRIMORDIA 1 (LRP1)
831 (Singh et al., 2020). LRP1 overexpression lines had fewer emerged lateral roots, suggesting that
832 LRP1 functions to inhibit lateral root emergence. By examining a *proLRP1*::GUS reporter, we
833 found that *LRP1* expression was increased by ACC in lateral root primordia at all stages of
834 primordia development, and in emerged lateral root tips and in the innermost root cells of

835 primary and lateral roots (Figure 12). However, we examined two *lrp1* mutant alleles in the
836 presence and absence of ACC we observed that one mutant had reduced inhibition of lateral root
837 formation in response to ACC, while the other allele did not, which is inconsistent with the wild-
838 type gene functioning to control lateral root development under our growth conditions.

839 We examined mutants in several other TFs that were selected based on their
840 transcriptional responses to ACC in both this dataset and our prior ACC time course dataset
841 (Harkey et al., 2018), including ANAC058, MYB9, MYB52, and RAP2.6L (Supplemental
842 Figures 15, 16, and 17). We found subtle but statistically significant root phenotypes in these
843 mutants, with *anac058-1*, *myb52-1*, and *rap2.6l-1* having reduced lateral root densities in the
844 presence of ACC compared to Col-0, and *myb9-1* having increased primary root growth
845 compared to Col-0 in the absence of ACC. We also found that *myb52-1* had fewer root hairs than
846 Col-0 in both the presence and absence of ACC. We also examined these mutants for triple
847 response phenotypes in the presence and absence of several concentrations of ACC, finding
848 differences in phenotypes between seedlings grown under continuous light conditions and those
849 grown in the dark for four days prior to exposure to light. These findings suggested that some of
850 these TFs could be involved in the light-dependent pathway downstream of ethylene (Harkey et
851 al., 2019).

852 This study provides insight into the ETR1-mediated GRN controlling root growth and
853 development, narrowing the previously identified genes that are regulated by ethylene and ACC
854 into a group of transcripts that are regulated by ETR1 and/or EIN3. We examined the
855 transcriptional regulation of genes encoding ACC oxidases to understand this final step in
856 ethylene synthesis, which controls the balance of accumulation of the ACC precursor and the
857 ethylene product. We find that the *ACO* transcript abundance is regulated more strongly by ACC

858 than ethylene consistent with feed forward synthesis of ethylene when ACC accumulates, which
859 hints at an ethylene-independent role in the regulation of this gene family. This study also
860 provides a valuable dataset to allow researchers to further dissect the role of ETR1 in controlling
861 root responses to changes in both ethylene and the ethylene precursor, ACC.

862 **Methods**

863 ***Genotypes and plant growth conditions***

864 All mutants used in this study were in the Col-0 background. Both the *etr1-3* and *etr1-7*
865 alleles have been described previously (Guzmán and Ecker, 1990; Harkey et al., 2018; Hua and
866 Meyerowitz, 1998). The *etr1-7* (AT1G66340) mutant was obtained from Elliot Meyerowitz (Hua
867 and Meyerowitz, 1998). T-DNA insertion mutants were obtained from the Arabidopsis
868 Biological Resource Center for AT3G18400 (SALK_049205C), AT5G12330
869 (SAIL_402_G06/CS873836 and SALK_201247C), AT5G16770 (SALK_149765C),
870 AT1G17950 (SALK_138624C), and AT5G13330 (SALK_051006C); see Supplemental Table 5
871 for more information on these lines. The *pACO*::GFP-GUS reporters were prepared by Dr. John
872 Vaughan-Hirsh and shared by Dr. Bram Van de Poel (Houben et el. 2024). The *proLRP1*::GUS
873 reporter was obtained from ABRC (Estornell et al., 2018).

874 Plants were grown on 1× Murashige and Skoog medium (Caisson Laboratories), pH 5.6,
875 Murashige and Skoog vitamins, and 0.8% agar, buffered with 0.05% MES (Sigma), and
876 supplemented with 1% sucrose. After stratification for 72 hours at 4°C, plants were grown under
877 100-130 μmol m^{-2} s^{-1} continuous cool-white light.

878 For selecting a dose of ethylene for the RNA-Seq, Col-0 seedlings were treated on day
879 five after germination. For ACC treatment, the seedlings were transferred to a growth medium
880 containing 0 or 0.75 μM ACC for 24 hours before imaging. For ethylene treatment, plates were
881 placed in clear treatment tanks with constant flow-through of the indicated concentration of
882 ethylene for 24 hours before imaging.

883

884 ***Method for selecting time points for RNA-Seq analysis using a previous microarray study***

885 We developed an analysis approach to identify the subset of time points that contained
886 the most unique (i.e., not found in other time points) DE genes in response to ACC treatment
887 using our previously published time-course microarray study with ACC treated Col-0 roots
888 (Harkey et al. 2018). In that prior study, we examined transcriptional responses to 1 μM ACC
889 after 0, 0.5, 1, 2, 4, 8, 12, and 24 hours of treatment, which overlaid the timeline for ACC-
890 induced root hair initiation. To inform the selection of time points for the present study, we first
891 analyzed the prior microarray data to find DE genes for each individual time point compared to
892 time 0. We then performed a pairwise comparison of time points to determine the number of
893 overlapping DE genes between each time point (Supplemental Figure 2B) and the percent of DE
894 genes in a time point that overlapped with another time point (Supplemental Figure 2A). These
895 results revealed that treatment times of 1, 4, and 24 hours contained the most unique sets of
896 transcripts while also overlapping with the timing of root hair formation to capture early, middle,
897 and late developmental responses. Therefore, we chose to perform RNA-Seq using samples
898 treated with ACC or ethylene at three time points: 1 hour, to monitor rapid transcriptional
899 responses that precede developmental changes; 4 hours, where the most unique transcripts are
900 DE and root hair initiation and primary root elongation are increasing and decreasing,
901 respectively, in response to treatment; and 24 hours to identify transcripts linked to ethylene-
902 modulated lateral root regulation.

903 Microarray data (Harkey et al., 2018) was analyzed using limma (Ritchie et al., 2015).
904 Probes were first filtered for interquartile range (IQR), with anything less than 0.1 excluded from
905 further analysis. Time points were then compared to their time-matched controls; p-values were
906 adjusted using a Benjamini-Hochberg correction. Genes with an absolute $\log_2$FC greater than 0.5

907 and an adjusted p-value less than 0.05 were considered to be DE at that time point. The overlap
908 matrix was created by comparing the DE genes across the time points in a pair-wise manner.
909 Supplemental Figure 1A graphically illustrates the results of this analysis. For each
910 column, the percentage of DE genes at that time point (column) that are also DE in the time point
911 to which it was compared (row) is shown. The number of genes in each comparison that was
912 used to calculate the percentages can be seen in Supplemental Figure 1B. For example, the 2-
913 hour time point showed considerable overlap with the four-hour time point; 87% of all 2-hour
914 DE genes were also DE at 4 hours. The reverse comparison of the four-hour genes that were also
915 DE at 2 hours yielded only 32% of the four-hour genes that were DE at two hours because there
916 were more DE genes in this 4-hour sample. Therefore, the four-hour time point identified nearly
917 all the same DE genes as the 2-hour time point, as well as many more unique genes, so we
918 selected the 4-hour time point over the 2-hour for this RNA-Seq analysis. We also examined the
919 overlaps of the 4- and 8-hour time points and the 12- and 24-hour time points, finding more
920 unique DE transcripts in the 8- and 24-hour time points for each of these overlaps. However, as
921 root hairs had already begun to initiate by 4 hours (Harkey et al., 2018), and the ethylene-
922 dependent inhibition of lateral root initiation had begun by 24 hours, these time points also
923 represented important developmental milestones. Ultimately, this analysis informed our choice to
924 do the present experiment with time points 0, 1, 4, and 24 hours.
925
926 ***ACC and ethylene treatment of seedlings for RNA isolation for sequencing***
927 Plants were grown on media as described above on top of a nylon filter (03-100/32; Sefar
928 Filtration) pressed against the plate, as described previously (Harkey et al., 2018; Levesque et al.,
929 2006). Approximately 100 sterilized seeds were placed on each filter; 2 plates were combined for

930 each biological replicate. ACC-treated samples were grown and harvested at Wake Forest
931 University, and ethylene-treated samples were grown and harvested at the University of
932 Tennessee Knoxville utilizing a gas flow-through system to treat with constant levels of ethylene
933 gas. The same researchers prepared both sets of samples, and identical reagents and light
934 treatments were used in both laboratories. Time-0 controls were prepared in both locations to
935 account for any location-specific effects on baseline expression.

936 Plants were treated on day five after germination. For time-0 samples, the nylon filter
937 containing five-day-old plants was transferred to a new control medium and root tissue was
938 immediately harvested. For ACC treatment, the plants on nylon were transferred to growth
939 medium with 1 μM ACC for the given treatment time (1, 4, and 24 h) and then root tissue was
940 harvested. For ethylene treatment, the nylon was transferred to new control medium, and plants
941 were placed in clear treatment tanks with constant flow-through of 0.3 ppm ethylene gas for the
942 given treatment time (1, 4, and 24 h) and then root tissue was harvested. At time of harvesting,
943 roots were cut from seedlings and flash frozen in liquid nitrogen. Frozen samples were ground in
944 liquid nitrogen, and RNA isolation was performed according to the Qiagen plant RNeasy kit
945 protocol, with the addition of the Qiagen RNase-free DNase treatment (Qiagen). After RNA
946 isolation, samples were quantified by A260 using a Nanodrop spectrophotometer (Nanodrop
947 Technologies). Each sample yielded at least 3 μg, and on average 15 μg, of RNA. One Col-0
948 sample which had a 4-hour ethylene treatment had an RNA integrity number (RIN) less than 6
949 and was not sequenced. Sequencing was performed by GENEWIZ, LLC using the Illumina
950 HiSeq platform.

951

952 ***RNA-Seq preprocessing and quality control***

953 FastQC v0.11.8 (Wingett and Andrews, 2018) and MultiQC v1.7 (Ewels et al., 2016)
954 were used for assessing read quality, which identified adaptor contamination and a bimodal GC
955 Content distribution. Adaptors were trimmed from reads using CutAdapt v1.18 (Martin, 2011),
956 and reads trimmed to less than 25 bp were removed. Trimmed reads were then processed with
957 the BBMap tool BBDuk (Bushnell 2014) to identify and remove rRNA contamination. Running
958 FastQC/MultiQC over the trimmed and filtered reads revealed the identified quality issues had
959 been mitigated. Read quantification was performed directly on the processed fastq files with the
960 Salmon v0.12.0 (Patro et al., 2017) "quant" algorithm in mapping mode using the "--
961 validateMapping" flag, setting the library type to "IU", and using the TAIR10 reference
962 transcriptome (NCBI ID: GCF_000001735.3). Counts were imported into R v3.6.0 using the
963 tximport R package v1.12.3 (Soneson et al., 2016) and summarized to the gene level.
964
965 ***Differential expression and visualization***
966 For visualization and sample comparisons, raw read counts were normalized using the
967 Variant Stabilizing Transformation method from the R package DESeq2 v1.24.0 (Love et al.,
968 2014). Sample-wise comparison heatmaps were generated using Pearson's correlation and
969 Euclidean distance as the distance metrics, respectively. PCA analyses were performed by
970 DESeq2's plotPCA method using the top 1000 most variable genes for all genotypes together,
971 and on a per-genotype basis.
972 All sample-wise comparisons were performed using the DESeq2 package and ashr v2.2-
973 47 (Stephens et al., 2020). Density plots were generated using ggplot2 v3.3.0 (Wickham, 2016),
974 and heatmaps of sample-wise comparisons were generated using ComplexHeatmap v.2.3.4 (Gu

975 et al., 2016). For DE transcripts used in heatmaps and GO analyses, we considered a transcript to
976 be DE if it had a p-value < 0.01, |logFC| > 0.5, and baseMean > 10.
977
978 ***Identification of outlier and pooling of control samples***
979 We performed ACC treatments at Wake Forest University and ethylene treatments at the
980 University of Tennessee. Therefore, to determine if these samples were similar, we first
981 compared the controls from each location for each genotype (Supplemental Table 1). Since the
982 controls for Col-0 and *etr1-3* were well matched between the two locations, and the PCA plots
983 suggested differences in *etr1-7* were not location dependent (Figure 2D), we combined the six
984 control (0-hour) samples for each genotype, or the five control samples for Col-0, excluding the
985 outlier sample described above, to use as the baseline for comparisons for the remaining
986 analyses.
987 To determine if all the Col-0 control (time-0) samples could be pooled for downstream
988 analyses, we generated a PCA plot using only the Col-0 samples (Supplemental Figure 3). This
989 plot revealed that one sample (in the ethylene time-0 treatment group) did not cluster with the
990 other control samples. This sample showed substantial separation from the rest along the PC1
991 axis, which represents over 50% of the variance across all the Col-0 samples. This outlier sample
992 was found to have far lower RNA yield than the other 71 samples, so we removed it from
993 downstream analyses. We generated a new PCA plot without this sample, revealing much greater
994 consistency.
995 To further validate this method, we performed two DE analyses to examine batch effects
996 on samples collected in the two locations, one with all six Col-0 control samples included (three
997 from each location) and one with the outlier sample removed. When all six samples were

998 included, 693 genes were found to be DE (adjusted p-value < 0.01, $|\log_2 FC| > 0.5$) between the
999 ACC and ethylene controls performed at these two locations (Supplemental Table 1). When the
1000 outlier sample identified by the PCA plot was removed from the analysis, only 34 genes were
1001 found to be DE between the Col-0 samples (Supplemental Table 1). This removal also affected
1002 the model generated by DESeq2, resulting in subtle effects on the *etr1-3* and *etr1-7* comparisons
1003 (Supplemental Table 1). In the model with the outlier Col-0 removed, 121 and 763 genes were
1004 DE between the controls compared at each location in *etr1-3* and *etr1-7*, respectively
1005 (Supplemental Table 1). The time-0 *etr1-7* samples had more DE genes between locations than
1006 had been expected, but there were two controls that were quite different than other samples (as
1007 evident in the PCA analysis in Figure 2D), which suggested that this is a character of two
1008 samples rather than a difference in samples because of location. We ultimately decided to
1009 combine the control samples for each genotype from both locations.

1010 ***PaLD analysis***

1011 A newly developed tool called Partitioned Local Depths (PaLD) was used to generate
1012 networks of the 553 ETR1-dependent transcripts and the 60 ETR1-dependent transcription
1013 factors, with application of this algorithm to gene expression and time course datasets described
1014 previously (Berenhaut et al., 2022; Khoury et al., 2024a). We sorted genes based on their
1015 transcript abundance patterns in response to ACC and ethylene over time in Col-0, *etr1-3*, and
1016 *etr1-7*. We used the $\log_2 FC$ values relative to time-0 Col-0 as input for the PaLD analysis. We
1017 further divided the networks using the Louvain method for community detection (Blondel et al.,
1018 2008). Relevant R code can be found at https://github.com/moorekatherine/pald.

1019 ***RT-qPCR***

1020 RNA was extracted from roots using the RNeasy Plant Mini Kit (Qiagen) according to
1021 the manufacturer's protocol, with buffer RLT selected as the extraction buffer for roots. RNA
1022 with A260/230 values less than 1.5 were re-isolated using isopropanol. DNA was removed using
1023 the RapidOut DNA Removal Kit (ThermoScientific) according to the manufacturer's
1024 instructions. Complementary DNA was synthesized using the Superscript III First-Strand
1025 Synthesis System for RT-PCR (Invitrogen) with RNA template primed with random hexamers
1026 according to the manufacturer's instructions. PowerUp SYBR Green Master Mix (Applied
1027 Biosystems) was used for quantitative PCR on a QuantStudio 3 Real-Time PCR System
1028 (Applied Biosystems). Primer efficiency and transcript abundance values were calculated using
1029 the standard curve method and primer sequence is reported in Supplemental Table 1.

1030 ***Fluorescence and brightfield imaging***

1031 For high resolution imaging of all *pACO*::GFP-GUS reporters, a Zeiss LSM 880
1032 microscope was used. Roots were first stained with propidium iodide (PI) diluted in water to a
1033 final concentration of 0.01 mg/mL for 2 min before being washed briefly in DI water and
1034 mounted on slides in DI water with #1.5 coverslips. Confocal images were acquired with a 488
1035 nm excitation laser for imaging GFP and the 561 nm laser for imaging PI with emission ranges
1036 of 490-552 nm and 56-696 nm, respectively. To minimize light scatter and improve image
1037 resolution, the pinholes for imaging GFP and PI were adjusted to slightly less than 1 Airy Unit.
1038 Images were taken with a Plan-Apo 20x/0.8NA objective and field size of 2048 x 2048 pixels.
1039 For Z-stacks, pixel dwell time was 0.26 µs and line averaging was set to 4. Z-stacks were
1040 obtained with 2.9 µm intervals between optical slices. For single-slice, high-resolution images,
1041 pixel dwell time was 1.02 µs and line averaging was set to 8.

1042 For epifluorescence imaging of the *pACO5*::GFP-GUS reporter, a Zeiss Axio Zoom.V16
1043 equipped with a PlanNeoFluar Z 1.0x (0.25NA) objective was used. An excitation range of 430-
1044 495 nm and emission range of 495-575 nm was employed with a Zeiss 38HE fluorescence filter
1045 cube. Images were captured with an Axiocam 506 monochrome camera with an exposure time of
1046 around 500 ms.

1047 For imaging *proLRP1*::GUS, the Zeiss Axio Zoom.V16 equipped with a PlanNeoFluar Z
1048 2.3x (0.75NA) objective was used. Images were captured with an AxioCam HR R3 color camera
1049 with an exposure time of around 10 ms.

1050 ***GUS staining procedure***

1051 Fresh X-Gluc (GoldBio) was dissolved on ice in N,N-Dimethylformamide immediately
1052 before incubating samples. For GUS staining, ten-day-old seedlings were vacuum infiltrated with
1053 GUS buffer containing X-Gluc (100 mM phosphate buffer pH 7, 0.5 mM $K_4Fe(CN)_6$, 0.5 mM,
1054 $K_3Fe(CN)_6$, 0.5 mM, 10 mM EDTA, 0.1% Triton X-100, and 2 mM X-Gluc) for five minutes,
1055 then incubated in the buffer and X-Gluc mixture for 1.5 hours at 37°C. Following product
1056 formation, seedlings were washed in 70% EtOH for 10 min. then fixed overnight in 3:1
1057 EtOH:acetic acid at 4°C in the dark prior to imaging.

1058 ***PCR genotyping***

1059 The primers used for genotyping are reported in Supplemental Table 5. Young leaf tissue
1060 was homogenized in a microcentrifuge tube using a micropestle that was dipped in liquid
1061 nitrogen. Edwards Solution (Edwards et al., 1991) was added to the homogenized leaf tissue and
1062 samples were incubated at room temperature for at least one hour before being spun down.
1063 Supernatant was carefully transferred to a new tube containing an equal volume of isopropanol.

1064 Samples were washed with EtOH and air dried in a sterile hood for approximately 30 minutes
1065 before being resuspended in molecular biology grade H_2O. Genotype was determined using
1066 wild-type primers that flanked the T-DNA insert (the wild-type reaction) to amplify the gene,
1067 and right border primers with T-DNA primers (the T-DNA reaction) to amplify the T-DNA
1068 insert (O'Malley et al., 2015), with primer sequences listed in Supplemental Table 5. DreamTaq
1069 DNA Polymerase (ThermoFisher) was used according to the manufacturer's instructions.

1070 ***Root development analysis***

1071 For analysis of root hair and lateral root phenotypes, five-day-old seedlings were
1072 transferred to plates containing 0 or 0.75 μM ACC for 4 hours or 5 days before imaging root
1073 hairs and lateral roots, respectively. For the root length analysis of dark grown seedlings, seeds
1074 were germinated in the dark for 4 days on untreated plates or plates containing 0.1, 0.2, 0.5, 1 or
1075 2 μM ACC, then root lengths were measured. Statistical tests (two-way ANOVA and multiple
1076 comparisons tests) were performed in GraphPad Prism 8.0.2. Outliers were identified using
1077 ROUT (Q = 1%).

1078

1079 **Acknowledgements**

1080 This work was supported by the National Science Foundation Systems and Synthetic Biology
1081 (MCB-1716279 to GKM) and the Center for Molecular Signaling Graduate Research Fellowship
1082 to MGW and a WFU Provost's Pilot Research grant (to GKM and MGW). We appreciate the
1083 help and mentorship of Megan Gerber, particularly the comparison of transcriptomic datasets.

1084

1085 **Author Contributions:**

Maleana White, Alexandria Harkey, and Amy Olex helped design the research, performed and analyzed data and wrote and edited the manuscript. Joelle Muhlemann, Nathan Pfeffer, and Maarten Houben performed experiments, analyzed data, and edited the manuscript. Brad Binder helped design and performed experiments and edited the manuscript. Gloria Muday designed experiments and wrote and edited the manuscript.

References

Abeles, F. B., Morgan, P. W., and Saltveit, M. E. (1992). *Ethylene in plant biology* (2nd ed). Academic Press.

Alonso, J. M., Hirayama, T., Roman, G., Nourizadeh, S., and Ecker, J. R. (1999). EIN2, a Bifunctional Transducer of Ethylene and Stress Responses in Arabidopsis. *Science*, *284*(5423), 2148–2152. https://doi.org/10.1126/science.284.5423.2148

Alonso, J. M., and Stepanova, A. N. (2004). The Ethylene Signaling Pathway. *Science*, *306*(5701), 1513–1515. https://doi.org/10.1126/science.1104812

Althiab-Almasaud, R., Sallanon, H., Chang, C., and Chervin, C. (2021). 1-Aminocyclopropane-1-carboxylic acid stimulates tomato pollen tube growth independently of ethylene receptors. *Physiologia Plantarum*, *173*(4), 2291–2297. https://doi.org/10.1111/ppl.13579

An, F., Zhao, Q., Ji, Y., Li, W., Jiang, Z., Yu, X., Zhang, C., Han, Y., He, W., Liu, Y., Zhang, S., Ecker, J. R., and Guo, H. (2010). Ethylene-Induced Stabilization of ETHYLENE INSENSITIVE3 and EIN3-LIKE1 Is Mediated by Proteasomal Degradation of EIN3 Binding F-Box 1 and 2 That Requires EIN2 in Arabidopsis. *The Plant Cell*, *22*(7), 2384–2401. https://doi.org/10.1105/tpc.110.076588

Azhar, B. J., Zulfiqar, A., Shakeel, S. N., and Schaller, G. E. (2020). Amplification and Adaptation in the Ethylene Signaling Pathway. *Small Methods*, *4*(8), 1900452. https://doi.org/10.1002/smtd.201900452

Berenhaut, K. S., Moore, K. E., and Melvin, R. L. (2022). A social perspective on perceived distances reveals deep community structure. *Proceedings of the National Academy of Sciences*, *119*(4), Article 4. https://doi.org/10.1073/pnas.2003634119

1113 Berleth, M., Berleth, N., Minges, A., Hänsch, S., Burkart, R. C., Stork, B., Stahl, Y.,
1114 Weidtkamp-Peters, S., Simon, R., and Groth, G. (2019). Molecular Analysis of Protein-
1115 Protein Interactions in the Ethylene Pathway in the Different Ethylene Receptor
1116 Subfamilies. *Frontiers in Plant Science*, *10*. https://www.frontiersin.org/journals/plant-
1117 science/articles/10.3389/fpls.2019.00726
1118 Binder, B. M. (2020). Ethylene signaling in plants. *The Journal of Biological Chemistry*,
1119 *295*(22), 7710–7725. PubMed. https://doi.org/10.1074/jbc.REV120.010854
1120 Binder, B. M., O'Malley, R. C., Wang, W., Zutz, T. C., and Bleecker, A. B. (2006). Ethylene
1121 Stimulates Nutations That Are Dependent on the ETR1 Receptor. *Plant Physiology*,
1122 *142*(4), 1690–1700. https://doi.org/10.1104/pp.106.087858
1123 Blondel, V. D., Guillaume, J.-L., Lambiotte, R., and Lefebvre, E. (2008). Fast unfolding of
1124 communities in large networks. *Journal of Statistical Mechanics: Theory and*
1125 *Experiment*, *2008*(10), Article 10. https://doi.org/10.1088/1742-5468/2008/10/P10008
1126 Brady, S. M., Orlando, D. A., Lee, J.-Y., Wang, J. Y., Koch, Dinneny, J. R., Mace, D., Ohler, U.,
1127 and Benfey, P. N. (2007). A High-Resolution Root Spatiotemporal Map Reveals
1128 Dominant Expression Patterns. *Science*, *318*(5851), 801–806.
1129 https://doi.org/10.1126/science.1146265
1130 Cancel, J. D., and Larsen, P. B. (2002). Loss-of-Function Mutations in the Ethylene
1131 ReceptorETR1 Cause Enhanced Sensitivity and Exaggerated Response to Ethylene in
1132 Arabidopsis. *Plant Physiology*, *129*(4), 1557–1567. https://doi.org/10.1104/pp.003780
1133 Chang, K. N., Zhong, S., Weirauch, M. T., Hon, G., Pelizzola, M., Li, H., Huang, S. C., Schmitz,
1134 R. J., Urich, M. A., Kuo, D., Nery, J. R., Qiao, H., Yang, A., Jamali, A., Chen, H., Ideker,
1135 T., Ren, B., Bar-Joseph, Z., Hughes, T. R., and Ecker, J. R. (2013). Temporal

1136 transcriptional response to ethylene gas drives growth hormone cross-regulation in
1137 Arabidopsis. *eLife*, *2*, e00675. https://doi.org/10.7554/eLife.00675
1138 Chang, Kwok, S. F., Bleecker, A. B., and Meyerowitz, E. M. (1993). Arabidopsis Ethylene-
1139 Response Gene ETR1: Similarity of Product to Two-Component Regulators. *Science*,
1140 *262*(5133), 539–544. https://doi.org/10.1126/science.8211181
1141 Davuluri, R. V., Sun, H., Palaniswamy, S. K., Matthews, N., Molina, C., Kurtz, M., and
1142 Grotewold, E. (2003). AGRIS: Arabidopsis Gene Regulatory Information Server, an
1143 information resource of Arabidopsis cis-regulatory elements and transcription factors.
1144 *BMC Bioinformatics*, *4*(1), 25. https://doi.org/10.1186/1471-2105-4-25
1145 Dolgikh, V. A., Pukhovaya, E. M., and Zemlyanskaya, E. V. (2019). Shaping Ethylene
1146 Response: The Role of EIN3/EIL1 Transcription Factors. *Frontiers in Plant Science*, *10*,
1147 1030. https://doi.org/10.3389/fpls.2019.01030
1148 Du, Z., Zhou, X., Ling, Y., Zhang, Z., and Su, Z. (2010). agriGO: a GO analysis toolkit for the
1149 agricultural community. *Nucleic Acids Research*, *38*(suppl_2), W64–W70.
1150 https://doi.org/10.1093/nar/gkq310
1151 Edwards, K., Johnstone, C., and Thompson, C. (1991). A simple and rapid method for the
1152 preparation of plant genomic DNA for PCR analysis. *Nucleic Acids Research*, *19*(6),
1153 1349–1349. https://doi.org/10.1093/nar/19.6.1349
1154 Estornell, L. H., Landberg, K., Cierlik, I., and Sundberg, E. (2018). SHI/STY Genes Affect Pre-
1155 and Post-meiotic Anther Processes in Auxin Sensing Domains in Arabidopsis. *Frontiers*
1156 *in Plant Science*, *9*. https://www.frontiersin.org/journals/plant-
1157 science/articles/10.3389/fpls.2018.00150

1158 Ewels, P., Magnusson, M., Lundin, S., and Käller, M. (2016). MultiQC: summarize analysis
1159 results for multiple tools and samples in a single report. *Bioinformatics*, *32*(19), 3047–
1160 3048. https://doi.org/10.1093/bioinformatics/btw354
1161 Feng, Y., Xu, P., Li, B., Li, P., Wen, X., An, F., Gong, Y., Xin, Y., Zhu, Z., Wang, Y., and Guo,
1162 H. (2017). Ethylene promotes root hair growth through coordinated EIN3/EIL1 and
1163 RHD6/RSL1 activity in Arabidopsis. *Proceedings of the National Academy of Sciences of*
1164 *the United States of America*, *114*(52), 13834–13839. PubMed.
1165 https://doi.org/10.1073/pnas.1711723115
1166 Fu, L., Liu, Y., Qin, G., Wu, P., Zi, H., Xu, Z., Zhao, X., Wang, Y., Li, Y., Yang, S., Peng, C.,
1167 Wong, C. C. L., Yoo, S.-D., Zuo, Z., Liu, R., Cho, Y.-H., and Xiong, Y. (2021). The
1168 TOR–EIN2 axis mediates nuclear signalling to modulate plant growth. *Nature*,
1169 *591*(7849), 288–292. https://doi.org/10.1038/s41586-021-03310-y
1170 Ge, S. X., Jung, D., and Yao, R. (2020). ShinyGO: a graphical gene-set enrichment tool for
1171 animals and plants. *Bioinformatics*, *36*(8), 2628–2629.
1172 https://doi.org/10.1093/bioinformatics/btz931
1173 Gu, Z., Eils, R., and Schlesner, M. (2016). Complex heatmaps reveal patterns and correlations in
1174 multidimensional genomic data. *Bioinformatics*, *32*(18), Article 18.
1175 https://doi.org/10.1093/bioinformatics/btw313
1176 Guzmán, P., and Ecker, J. R. (1990). Exploiting the triple response of Arabidopsis to identify
1177 ethylene-related mutants. *The Plant Cell*, *2*(6), 513–523.
1178 https://doi.org/10.1105/tpc.2.6.513
1179 Harkey, A. F., Watkins, J. M., Olex, A. L., DiNapoli, K. T., Lewis, D. R., Fetrow, J. S., Binder,
1180 B. M., and Muday, G. K. (2018). Identification of Transcriptional and Receptor Networks

1181 That Control Root Responses to Ethylene. *Plant Physiology*, *176*(3), 2095–2118.
1182 https://doi.org/10.1104/pp.17.00907
1183 Harkey, A. F., Yoon, G. M., Seo, D. H., DeLong, A., and Muday, G. K. (2019). Light Modulates
1184 Ethylene Synthesis, Signaling, and Downstream Transcriptional Networks to Control
1185 Plant Development. *Frontiers in Plant Science*, *10*, 1094.
1186 https://doi.org/10.3389/fpls.2019.01094
1187 Houben, M., and Van de Poel, B. (2019). 1-Aminocyclopropane-1-Carboxylic Acid Oxidase
1188 (ACO): The Enzyme That Makes the Plant Hormone Ethylene. *Frontiers in Plant*
1189 *Science*, *10*. https://www.frontiersin.org/articles/10.3389/fpls.2019.00695
1190 Houben, M., Vaughan-Hirsch, J., Pattyn, J., Mou, W., Roden, S., Martinez Roig, A., Kabak, E.,
1191 Rodrigues, S., Polko, A., De Coninck, B., Kieber, J. J., Voet, A., and Van de Poel, B.
1192 (2024). 1-Aminocyclopropane-1-carboxylic acid oxidase determines the fate of ethylene
1193 biosynthesis in a tissue-specific way to fine-tune development and stress resilience.
1194 *bioRxiv*, 2024.02.01.578397. https://doi.org/10.1101/2024.02.01.578397
1195 Hua, J., and Meyerowitz, E. M. (1998). Ethylene Responses Are Negatively Regulated by a
1196 Receptor Gene Family in Arabidopsis thaliana. *Cell*, *94*(2), 261–271.
1197 https://doi.org/10.1016/S0092-8674(00)81425-7
1198 Hua, J., Sakai, H., Nourizadeh, S., Chen, Q. G., Bleecker, A. B., Ecker, J. R., and Meyerowitz, E.
1199 M. (1998). EIN4 and ERS2 Are Members of the Putative Ethylene Receptor Gene Family
1200 in Arabidopsis. *The Plant Cell*, *10*(8), 1321–1332. https://doi.org/10.1105/tpc.10.8.1321
1201 Huang, Y., Li, H., Hutchison, C. E., Laskey, J., and Kieber, J. J. (2003). Biochemical and
1202 functional analysis of CTR1, a protein kinase that negatively regulates ethylene signaling

in Arabidopsis. *The Plant Journal*, *33*(2), 221–233. https://doi.org/10.1046/j.1365-313X.2003.01620.x

Ivanchenko, M. G., Muday, G. K., and Dubrovsky, J. G. (2008). Ethylene–auxin interactions regulate lateral root initiation and emergence in Arabidopsis thaliana. *The Plant Journal*, *55*(2), 335–347. https://doi.org/10.1111/j.1365-313X.2008.03528.x

Khoury, M. G., Berenhaut, K. S., Moore, K. E., Allen, E. E., Harkey, A. F., Mühlemann, J. K., Craven, C. N., Xu, J., Jain, S. S., John, D. J., Norris, J. L., and Muday, G. K. (2024). Informative community structure revealed using Arabidopsis time series transcriptome data via partitioned local depth. *In Silico Plants*, *6*(1), diad018. https://doi.org/10.1093/insilicoplants/diad018

Khoury, M. G., Martin, R. E., Houben, M., and Muday, G. K. (2024). Ethylene Regulates Root Growth and Development. In *Plant Roots: The Hidden Half* (5th ed.). CRC Press. 10.1201/b23126-19

Kieber, J. J., Rothenberg, M., Roman, G., Feldmann, K. A., and Ecker, J. R. (1993). CTR1, a negative regulator of the ethylene response pathway in arabidopsis, encodes a member of the Raf family of protein kinases. *Cell*, *72*(3), 427–441. https://doi.org/10.1016/0092-8674(93)90119-B

Kim, H., Helmbrecht, E. E., Stalans, M. B., Schmitt, C., Patel, N., Wen, C.-K., Wang, W., and Binder, B. M. (2011). Ethylene Receptor ETHYLENE RECEPTOR1 Domain Requirements for Ethylene Responses in Arabidopsis Seedlings. *Plant Physiology*, *156*(1), 417–429. https://doi.org/10.1104/pp.110.170621

1224 Lee, S. H., and Cho, H.-T. (2008). Auxin and Root Hair Morphogenesis. In *Plant Cell*
1225 *Monographs* (pp. 1–20). Springer Berlin Heidelberg.
1226 https://doi.org/10.1007/7089_2008_16
1227 Levesque, M. P., Vernoux, T., Busch, W., Cui, H., Wang, J. Y., Blilou, I., Hassan, H., Nakajima,
1228 K., Matsumoto, N., Lohmann, J. U., Scheres, B., and Benfey, P. N. (2006). Correction:
1229 Whole-Genome Analysis of the SHORT-ROOT Developmental Pathway in Arabidopsis.
1230 *PLOS Biology*, *4*(7), e249. https://doi.org/10.1371/journal.pbio.0040249
1231 Lewis, D. R., Negi, S., Sukumar, P., and Muday, G. K. (2011). Ethylene inhibits lateral root
1232 development, increases IAA transport and expression of PIN3 and PIN7 auxin efflux
1233 carriers. *Development*, *138*(16), 3485–3495. https://doi.org/10.1242/dev.065102
1234 Li, D., Flores-Sandoval, E., Ahtesham, U., Coleman, A., Clay, J. M., Bowman, J. L., and Chang,
1235 C. (2020). Ethylene-independent functions of the ethylene precursor ACC in Marchantia
1236 polymorpha. *Nature Plants*, *6*(11), 1335–1344. https://doi.org/10.1038/s41477-020-
1237 00784-y
1238 Li, D., Mou, W., Van de Poel, B., and Chang, C. (2022). Something old, something new:
1239 Conservation of the ethylene precursor 1-amino-cyclopropane-1-carboxylic acid as a
1240 signaling molecule. *Current Opinion in Plant Biology*, *65*, 102116.
1241 https://doi.org/10.1016/j.pbi.2021.102116
1242 Love, M. I., Huber, W., and Anders, S. (2014). Moderated estimation of fold change and
1243 dispersion for RNA-seq data with DESeq2. *Genome Biology*, *15*(12), 550.
1244 https://doi.org/10.1186/s13059-014-0550-8

1245 Ma, Q., and Dong, C.-H. (2021). Regulatory functions and molecular mechanisms of ethylene
1246 receptors and receptor-associated proteins in higher plants. *Plant Growth Regulation*,
1247 *93*(1), 39–52. https://doi.org/10.1007/s10725-020-00674-5
1248 Martin. (2011). Cutadapt removes adapter sequences from high-throughput sequencing reads.
1249 *EMBnet.Journal*, *17*, 10–12.
1250 Martin, R. E., Marzol, E., Estevez, J. M., and Muday, G. K. (2022). Ethylene signaling increases
1251 reactive oxygen species accumulation to drive root hair initiation in Arabidopsis.
1252 *Development*, *149*(13), dev200487. https://doi.org/10.1242/dev.200487
1253 Masucci, J. D., and Schiefelbein, J. W. (1996). Hormones act downstream of TTG and GL2 to
1254 promote root hair outgrowth during epidermis development in the Arabidopsis root. *The*
1255 *Plant Cell*, *8*(9), 1505–1517. https://doi.org/10.1105/tpc.8.9.1505
1256 McDaniel, B. K., and Binder, B. M. (2012). Ethylene Receptor 1 (ETR1) Is Sufficient and Has
1257 the Predominant Role in Mediating Inhibition of Ethylene Responses by Silver in
1258 Arabidopsis thaliana*. *Journal of Biological Chemistry*, *287*(31), 26094–26103.
1259 https://doi.org/10.1074/jbc.M112.383034
1260 Mou, W., Kao, Y.-T., Michard, E., Simon, A. A., Li, D., Wudick, M. M., Lizzio, M. A., Feijó, J.
1261 A., and Chang, C. (2020). Ethylene-independent signaling by the ethylene precursor ACC
1262 in Arabidopsis ovular pollen tube attraction. *Nature Communications*, *11*(1), 4082.
1263 https://doi.org/10.1038/s41467-020-17819-9
1264 Mou, W., Khare, R., Polko, J. K., Taylor, I., Xu, J., Xue, D., Benfey, P., Van de Poel, B., Chang,
1265 C., and Kieber, J. J. (2025). Ethylene-independent modulation of root development by
1266 ACC via downregulation of WOX5 and group I CLE peptide expression. *Proceedings of*

1267 *the National Academy of Sciences*, *122*(6), e2417735122.
1268 https://doi.org/10.1073/pnas.2417735122
1269 Muday, G. K., Rahman, A., and Binder, B. M. (2012). Auxin and ethylene: Collaborators or
1270 competitors? *Trends in Plant Science*, *17*(4), 181–195.
1271 https://doi.org/10.1016/j.tplants.2012.02.001
1272 Negi, S., Ivanchenko, M. G., and Muday, G. K. (2008). Ethylene regulates lateral root formation
1273 and auxin transport in Arabidopsis thaliana. *The Plant Journal*, *55*(2), 175–187.
1274 https://doi.org/10.1111/j.1365-313X.2008.03495.x
1275 O'Malley, R. C., Barragan, C. C., and Ecker, J. R. (2015). A user's guide to the Arabidopsis T-
1276 DNA insertion mutant collections. *Methods in Molecular Biology (Clifton, N.J.)*, *1284*,
1277 323–342. PubMed. https://doi.org/10.1007/978-1-4939-2444-8_16
1278 O'Malley, R. C., Huang, S.-S. C., Song, L., Lewsey, M. G., Bartlett, A., Nery, J. R., Galli, M.,
1279 Gallavotti, A., and Ecker, J. R. (2016). Cistrome and Epicistrome Features Shape the
1280 Regulatory DNA Landscape. *Cell*, *165*(5), 1280–1292. PubMed.
1281 https://doi.org/10.1016/j.cell.2016.04.038
1282 Palaniswamy, S. K., James, S., Sun, H., Lamb, R. S., Davuluri, R. V., and Grotewold, E. (2006).
1283 AGRIS and AtRegNet. A Platform to Link cis-Regulatory Elements and Transcription
1284 Factors into Regulatory Networks. *Plant Physiology*, *140*(3), 818–829.
1285 https://doi.org/10.1104/pp.105.072280
1286 Patro, R., Duggal, G., Love, M. I., Irizarry, R. A., and Kingsford, C. (2017). Salmon provides
1287 fast and bias-aware quantification of transcript expression. *Nature Methods*, *14*(4), 417–
1288 419. https://doi.org/10.1038/nmeth.4197

1289 Pires, N. D., Yi, K., Breuninger, H., Catarino, B., Menand, B., and Dolan, L. (2013).
1290 Recruitment and remodeling of an ancient gene regulatory network during land plant
1291 evolution. *Proceedings of the National Academy of Sciences*, *110*(23), 9571–9576.
1292 https://doi.org/10.1073/pnas.1305457110
1293 Polko, J. K., and Kieber, J. J. (2019). 1-Aminocyclopropane 1-Carboxylic Acid and Its Emerging
1294 Role as an Ethylene-Independent Growth Regulator. *Frontiers in Plant Science*, *10*.
1295 https://www.frontiersin.org/journals/plant-science/articles/10.3389/fpls.2019.01602
1296 Qiao, H., Chang, K. N., Yazaki, J., and Ecker, J. R. (2009). Interplay between ethylene,
1297 ETP1/ETP2 F-box proteins, and degradation of EIN2 triggers ethylene responses in
1298 Arabidopsis. *Genes & Development*, *23*(4), 512–521.
1299 Qin, H., He, L., and Huang, R. (2019). The Coordination of Ethylene and Other Hormones in
1300 Primary Root Development. *Frontiers in Plant Science*, *10*.
1301 https://www.frontiersin.org/articles/10.3389/fpls.2019.00874
1302 Rahman, A., Tsurumi, S., Amakawa, T., Soga, K., Hoson, T., Goto, N., and Kamisaka, S. (2000).
1303 Involvement of Ethylene and Gibberellin Signalings in Chromosaponin I-Induced Cell
1304 Division and Cell Elongation in the Roots of Arabidopsis Seedlings. *Plant and Cell*
1305 *Physiology*, *41*(1), 1–9. https://doi.org/10.1093/pcp/41.1.1
1306 Ritchie, M. E., Phipson, B., Wu, D., Hu, Y., Law, C. W., Shi, W., and Smyth, G. K. (2015).
1307 Limma powers differential expression analyses for RNA-sequencing and microarray
1308 studies. *Nucleic Acids Research*, *43*(7), Article 7. https://doi.org/10.1093/nar/gkv007
1309 Růžička, K., Ljung, K., Vanneste, S., Podhorská, R., Beeckman, T., Friml, J., and Benková, E.
1310 (2007). Ethylene Regulates Root Growth through Effects on Auxin Biosynthesis and

1311 Transport-Dependent Auxin Distribution. *The Plant Cell*, *19*(7), 2197–2212.
1312 https://doi.org/10.1105/tpc.107.052126
1313 Sakai, H., Hua, J., Chen, Q. G., Chang, C., Medrano, L. J., Bleecker, A. B., and Meyerowitz, E.
1314 M. (1998). ETR2 is an ETR1-like gene involved in ethylene signaling in Arabidopsis.
1315 *Proceedings of the National Academy of Sciences*, *95*(10), 5812–5817.
1316 https://doi.org/10.1073/pnas.95.10.5812
1317 Schaller, G. E., and Bleecker, A. B. (1995). Ethylene-Binding Sites Generated in Yeast
1318 Expressing the Arabidopsis ETR1 Gene. *Science*, *270*(5243), 1809–1811. JSTOR.
1319 Schaller, G. E., and Kieber, J. G. (2002). Ethylene. *The Arabidopsis Book*, *2002*(1).
1320 https://doi.org/10.1199/tab.0071
1321 Shakeel, S. N., Wang, X., Binder, B. M., and Schaller, G. E. (2013). Mechanisms of signal
1322 transduction by ethylene: Overlapping and non-overlapping signalling roles in a receptor
1323 family. *AoB PLANTS*, *5*, plt010. https://doi.org/10.1093/aobpla/plt010
1324 Singh, S., Yadav, S., Singh, A., Mahima, M., Singh, A., Gautam, V., and Sarkar, A. K. (2020).
1325 Auxin signaling modulates LATERAL ROOT PRIMORDIUM1 (LRP1) expression
1326 during lateral root development in Arabidopsis. *The Plant Journal*, *101*(1), 87–100.
1327 https://doi.org/10.1111/tpj.14520
1328 Soneson, C., Matthes, K. L., Nowicka, M., Law, C. W., and Robinson, M. D. (2016). Isoform
1329 prefiltering improves performance of count-based methods for analysis of differential
1330 transcript usage. *Genome Biology*, *17*(1), 12. https://doi.org/10.1186/s13059-015-0862-3
1331 Stepanova, A. N., Yun, J., Likhacheva, A. V., and Alonso, J. M. (2007). Multilevel Interactions
1332 between Ethylene and Auxin in *Arabidopsis* Roots. *The Plant Cell*, *19*(7), Article 7.
1333 https://doi.org/10.1105/tpc.107.052068

1334 Stephens, M., Carbonetto, P., Gerard, D., Lu, M., Sun, L., Willwerscheid, J., and Xiao, N.
1335 (2020). *Methods for Adaptive Shrinkage, using Empirical Bayes [R package ashr version*
1336 *2.2-47]*. https://api.semanticscholar.org/CorpusID:226047420
1337 Sukumar, P., Edwards, K. S., Rahman, A., DeLong, A., and Muday, G. K. (2009). PINOID
1338 Kinase Regulates Root Gravitropism through Modulation of PIN2-Dependent Basipetal
1339 Auxin Transport in Arabidopsis. *Plant Physiology*, *150*(2), 722–735.
1340 https://doi.org/10.1104/pp.108.131607
1341 Tian, T., Liu, Y., Yan, H., You, Q., Yi, X., Du, Z., Xu, W., and Su, Z. (2017). agriGO v2.0: A
1342 GO analysis toolkit for the agricultural community, 2017 update. *Nucleic Acids Research*,
1343 *45*(W1), Article W1. https://doi.org/10.1093/nar/gkx382
1344 Tsang, D. L., Edmond, C., Harrington, J. L., and Nühse, T. S. (2011). Cell Wall Integrity
1345 Controls Root Elongation via a General 1-Aminocyclopropane-1-Carboxylic Acid-
1346 Dependent, Ethylene-Independent Pathway. *Plant Physiology*, *156*(2), 596–604.
1347 https://doi.org/10.1104/pp.111.175372
1348 Tsuchisaka, A., Yu, G., Jin, H., Alonso, J. M., Ecker, J. R., Zhang, X., Gao, S., and Theologis,
1349 A. (2009). A Combinatorial Interplay Among the 1-Aminocyclopropane-1-Carboxylate
1350 Isoforms Regulates Ethylene Biosynthesis in Arabidopsis thaliana. *Genetics*, *183*(3),
1351 979–1003. https://doi.org/10.1534/genetics.109.107102
1352 Van de Poel, B. (2020). Ethylene's fraternal twin steals the spotlight. *Nature Plants*, *6*(11),
1353 1309–1310. https://doi.org/10.1038/s41477-020-00796-8
1354 Van de Poel, B., Smet, D., and Van Der Straeten, D. (2015). Ethylene and Hormonal Cross Talk
1355 in Vegetative Growth and Development. *Plant Physiology*, *169*(1), 61–72.
1356 https://doi.org/10.1104/pp.15.00724

1357 Van de Poel, B., and Van Der Straeten, D. (2014). 1-aminocyclopropane-1-carboxylic acid
1358 (ACC) in plants: More than just the precursor of ethylene! *Frontiers in Plant Science*, *5*.
1359 https://www.frontiersin.org/journals/plant-science/articles/10.3389/fpls.2014.00640
1360 Vanderstraeten, L., Depaepe, T., Bertrand, S., and Van Der Straeten, D. (2019). The Ethylene
1361 Precursor ACC Affects Early Vegetative Development Independently of Ethylene
1362 Signaling. *Frontiers in Plant Science*, *10*.
1363 https://www.frontiersin.org/articles/10.3389/fpls.2019.01591
1364 Wang, K. L.-C., Li, H., and Ecker, J. R. (2002). Ethylene Biosynthesis and Signaling Networks.
1365 *The Plant Cell*, *14*(suppl_1), S131–S151. https://doi.org/10.1105/tpc.001768
1366 Wickham, H. (2016). *ggplot2: Elegant Graphics for Data Analysis* (2nd ed.). Springer Cham.
1367 https://doi.org/10.1007/978-3-319-24277-4
1368 Wingett, S., and Andrews, S. (2018). FastQ Screen: A tool for multi-genome mapping and
1369 quality control [version 2; peer review: 4 approved]. *F1000Research*, *7*(1338).
1370 https://doi.org/10.12688/f1000research.15931.2
1371 Xu, S.-L., Rahman, A., Baskin, T. I., and Kieber, J. J. (2008). Two Leucine-Rich Repeat
1372 Receptor Kinases Mediate Signaling, Linking Cell Wall Biosynthesis and ACC Synthase
1373 in Arabidopsis. *The Plant Cell*, *20*(11), 3065–3079.
1374 https://doi.org/10.1105/tpc.108.063354
1375 Yin, J., Zhang, X., Zhang, G., Wen, Y., Liang, G., and Chen, X. (2019). Aminocyclopropane-1-
1376 carboxylic acid is a key regulator of guard mother cell terminal division in Arabidopsis
1377 thaliana. *Journal of Experimental Botany*, *70*(3), 897–908.
1378 https://doi.org/10.1093/jxb/ery413
1379

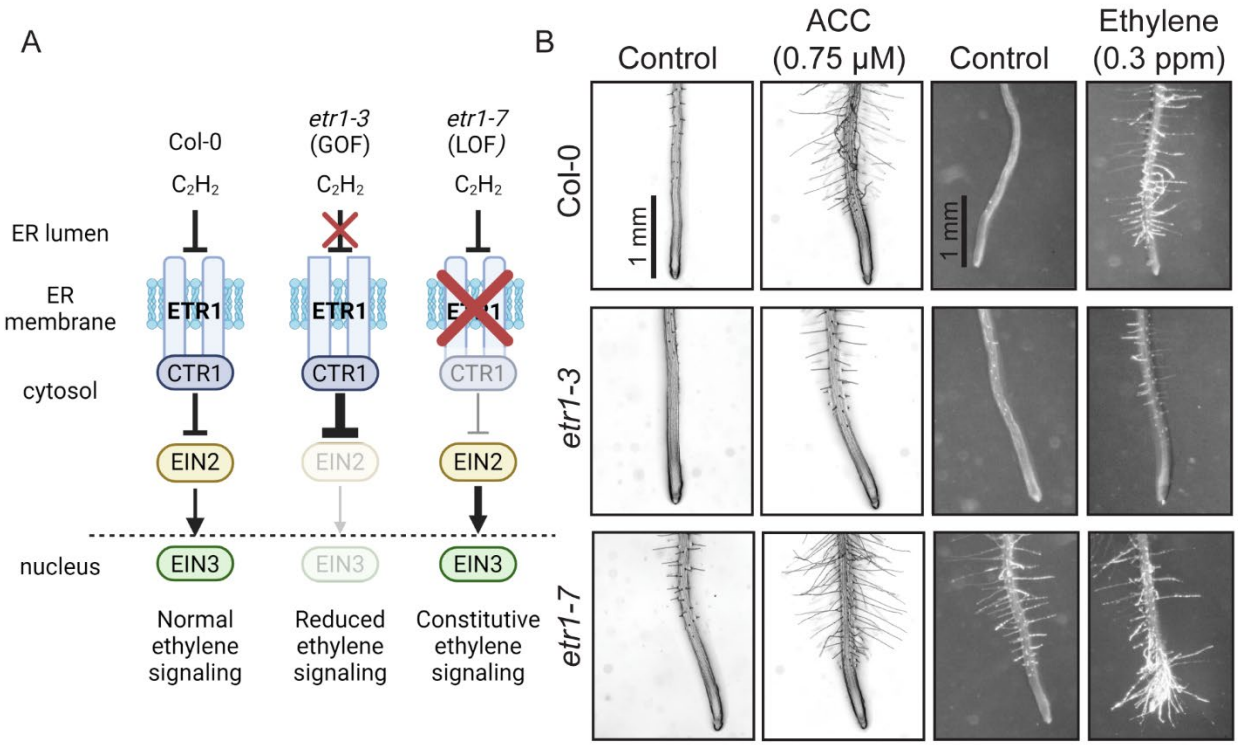

Figure 1. Altered ethylene signaling in the *etr1-3* and *etr1-7* mutants results in aberrant root hair formation. (A) A schematic illustrating the wild-type ethylene signaling pathway and how it is altered in *etr1-3* and *etr1-7* mutants. This image was prepared using Biorender. (B) Representative images of six-day-old Col-0, *etr1-3*, and *etr1-7* seedlings treated with 0.3 ppm ethylene or 0.75 μM ACC for 24 hours, revealing similar developmental responses by these two doses of ethylene and ACC within the different genotypes.

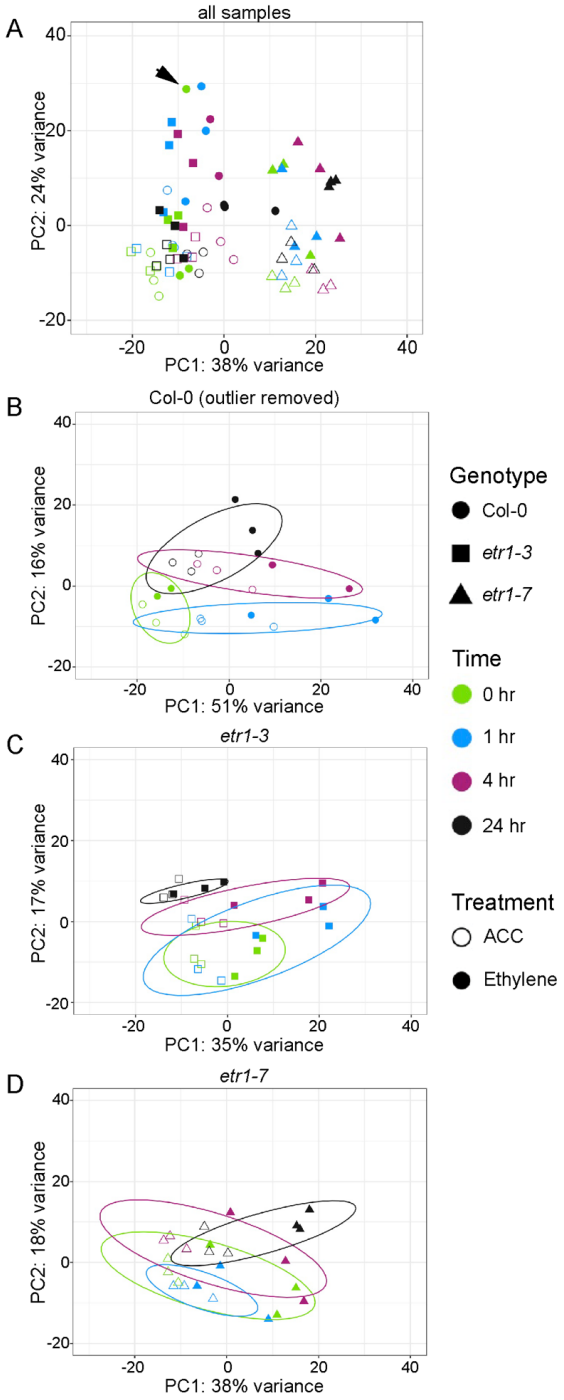

1387

1388 **Figure 2. Large-scale transcript abundance patterns in data show *etr1-7* samples are**
1389 **distinctly different from Col-0 and *etr1-3*.** (A) PCA plot of all sequenced samples with the
1390 genotype indicated by shape of the symbol, the time of treatment indicated by color, and the
1391 treatment type ACC or ethylene, indicated by open or filled symbols, respectively. The arrow
1392 denotes an untreated Col-0 outlier. PCA plots of (B) Col-0 (with the outlier sample removed),
1393 (C) *etr1-3*, and (D) *etr1-7* samples. Circles surround the 80% confidence intervals for each time
1394 point.

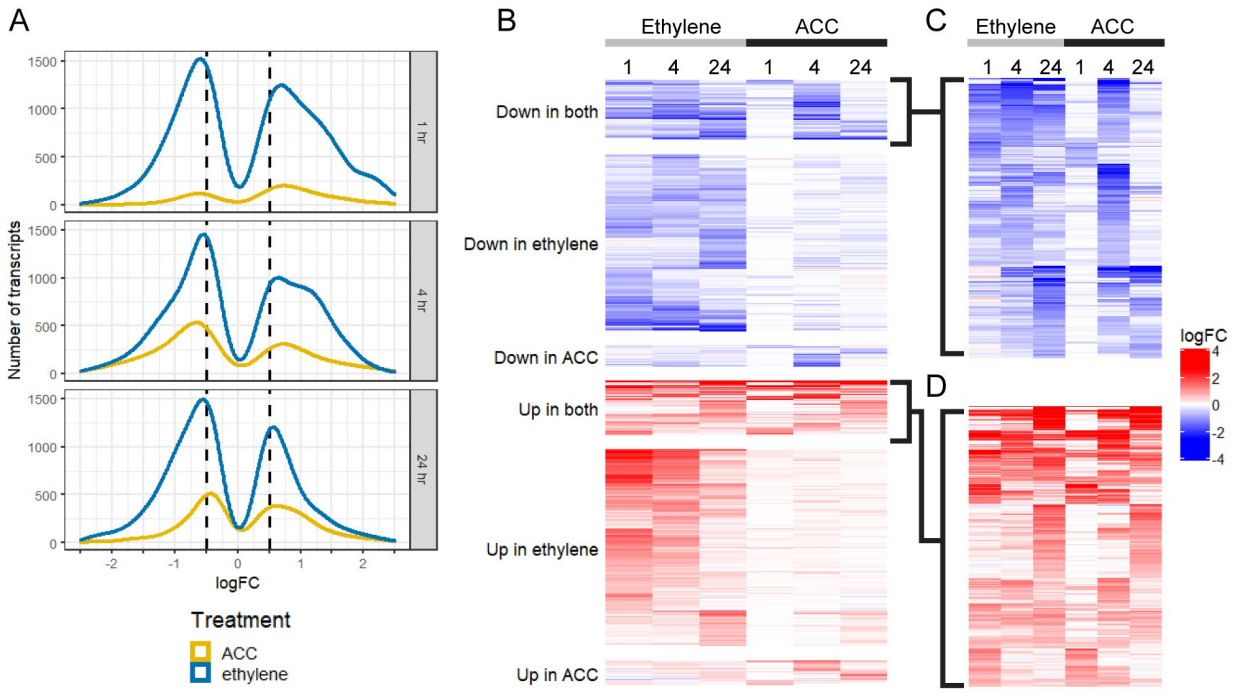

Figure 3. The transcriptional responses to ethylene and ACC treatment revealed more down-regulated genes at 4 and 24 hours and more DE genes by ethylene than ACC. (A) Density plot reporting the number of transcripts across a range of $\log_2$FC values for each treatment and time point in Col-0 samples. The $\log_2$FC is relative to Col-0 control (time 0). For each treatment and time point, only transcripts with an adjusted p-value < 0.01 are shown; no $\log_2$FC cutoff was used. (B) Heatmap showing the $\log_2$FC values of the 4,522 transcripts that were DE relative to untreated Col-0 in at least one Col-0 sample treated with ethylene or ACC based on $|\log_2\text{FC}| > 0.5$ and adjusted p-value < 0.01. (C & D) Transcripts which are DE in at least one time point for both ethylene and ACC, with a (C) negative or (D) positive $\log_2$FC.

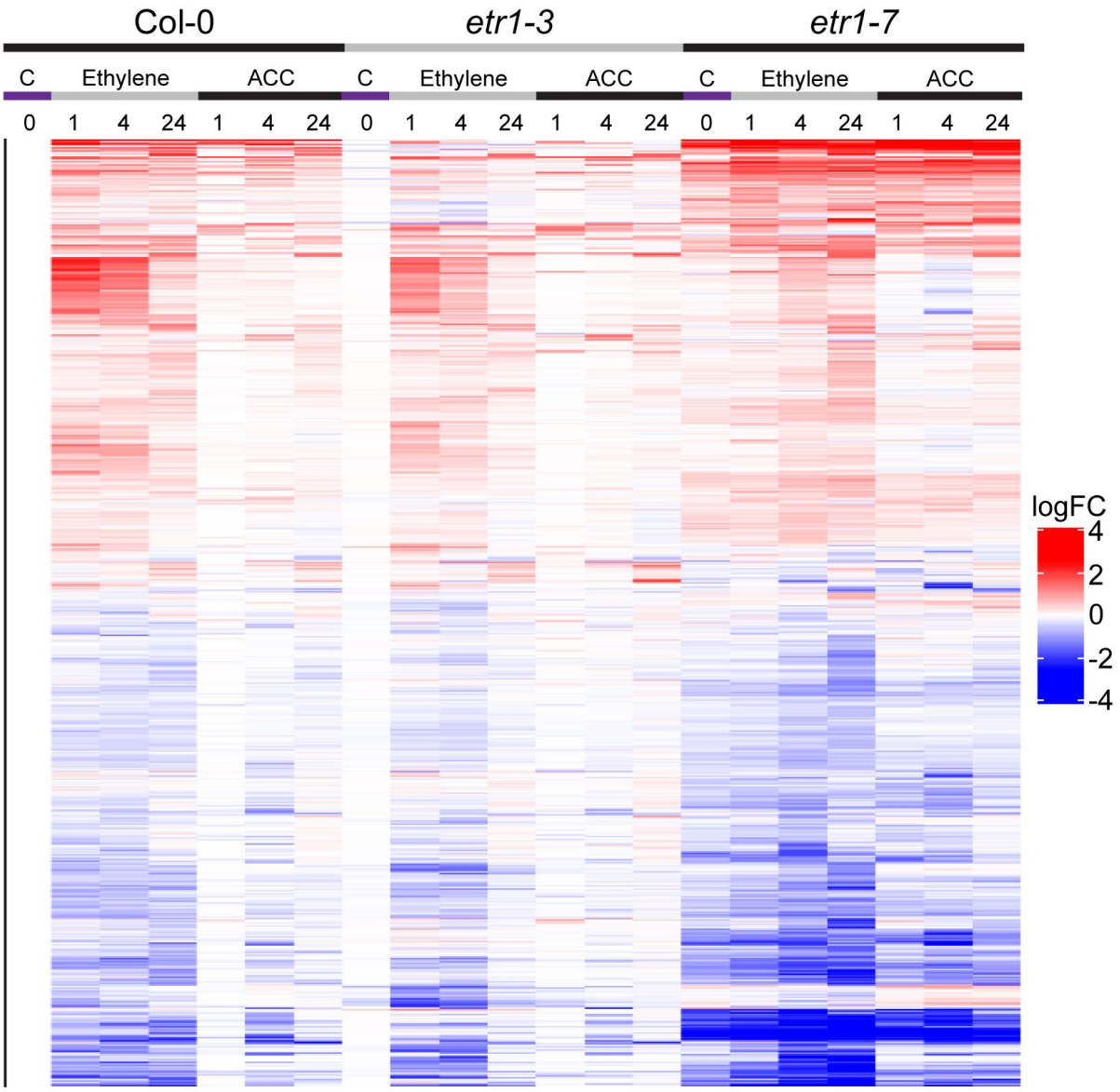

Figure 4. Heatmap of all transcripts that were DE in at least one time point, treatment, or genotype revealed a variety of patterns. This comparison of the transcriptional responses of 8,323 DE transcripts across treatments, time points and genotypes revealed suppressed ethylene signaling in *etr1-3* and enhanced ethylene signaling in *etr1-7*, relative to Col-0 untreated. The heat map includes all 8,323 transcripts that are DE in at least one of the represented groups in comparison with Col-0 control with $|\log_2 FC| > 0.5$ and adjusted p-value < 0.01. $\log_2 FC$ for all columns is relative to untreated Col-0 samples.

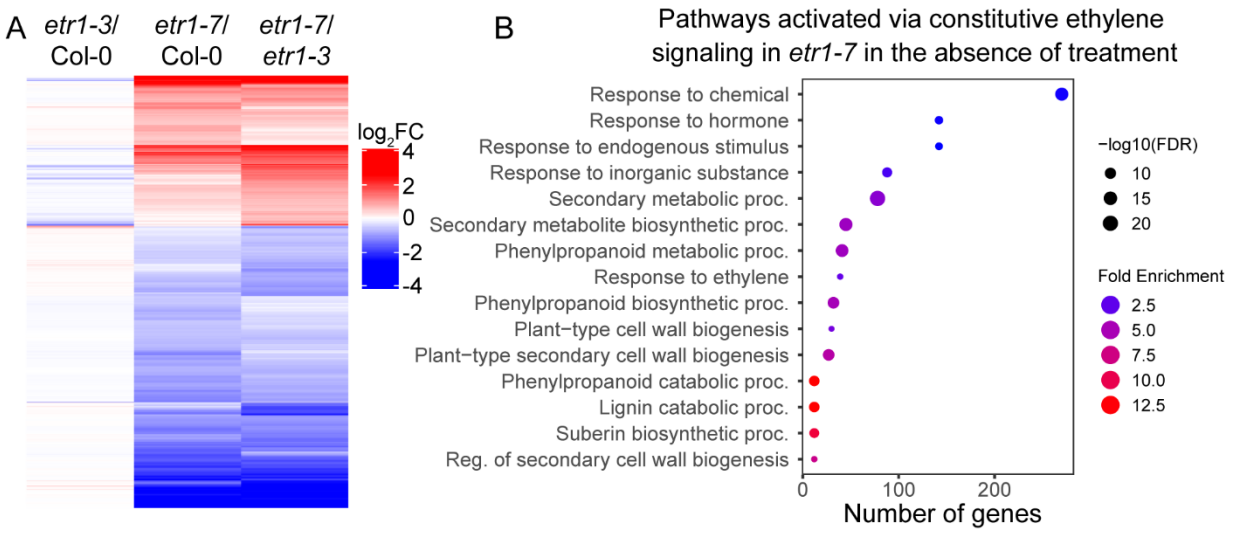

Figure 5. Baseline transcript abundance differences between Col-0 and the *etr1* mutants were consistent with constitutive ethylene signaling in *etr1-7*. (A) All transcripts which are DE in at least one comparison with $|\log_2 FC| > 0.5$ and adjusted p-value < 0.01. $\log_2 FC$ is relative to the second genotype in each comparison. (B) Enriched biological processes among the 1,458 DE genes in the overlap between the *etr1-7* vs. Col-0 comparisons and the *etr1-7* vs. *etr1-3* comparisons as determined by ShinyGO 0.80 (Ge et al., 2020).

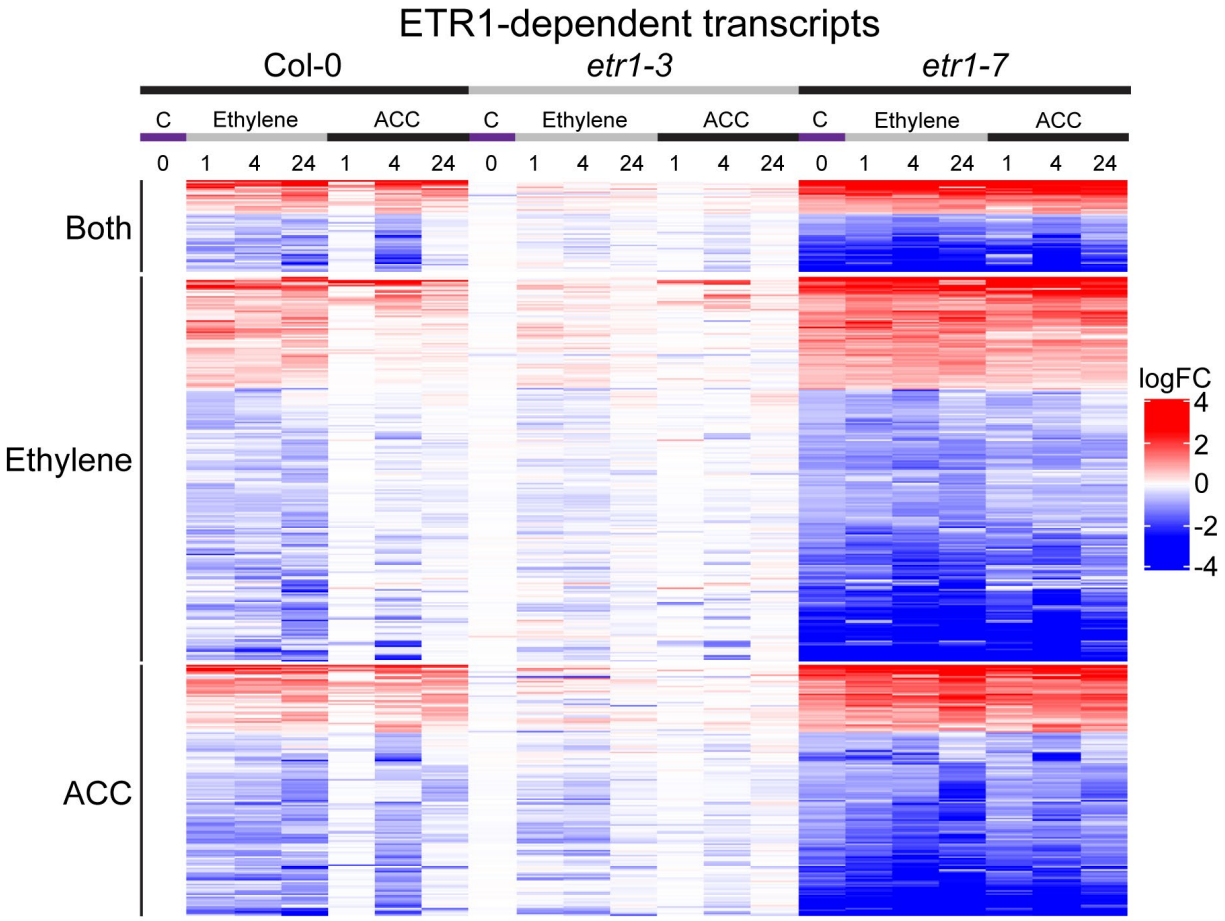

Figure 6. ETR1-dependent transcript heatmap revealed genotype and treatment dependent changes in transcript abundance. This comparison of transcript abundance across treatments and genotypes revealed a set of transcripts that responded to ethylene and/or ACC treatment in Col-0 but not in the mutants. Transcripts which follow a pattern of response that suggests they are ETR1-dependent were selected. These transcripts respond to ACC and/or ethylene treatment in Col-0, do not respond in *etr1-3*, and are constitutively up or down in *etr1-7*, based on $|\log_2 FC| > 0.5$ and adjusted p-value < 0.01. The $\log_2 FC$ reported here was determined relative to untreated Col-0. Genes are split into three groups based on whether they met our ETR1-dependent criteria in ethylene only (292 transcripts), ACC only (191 transcripts), or both treatments (70 transcripts).

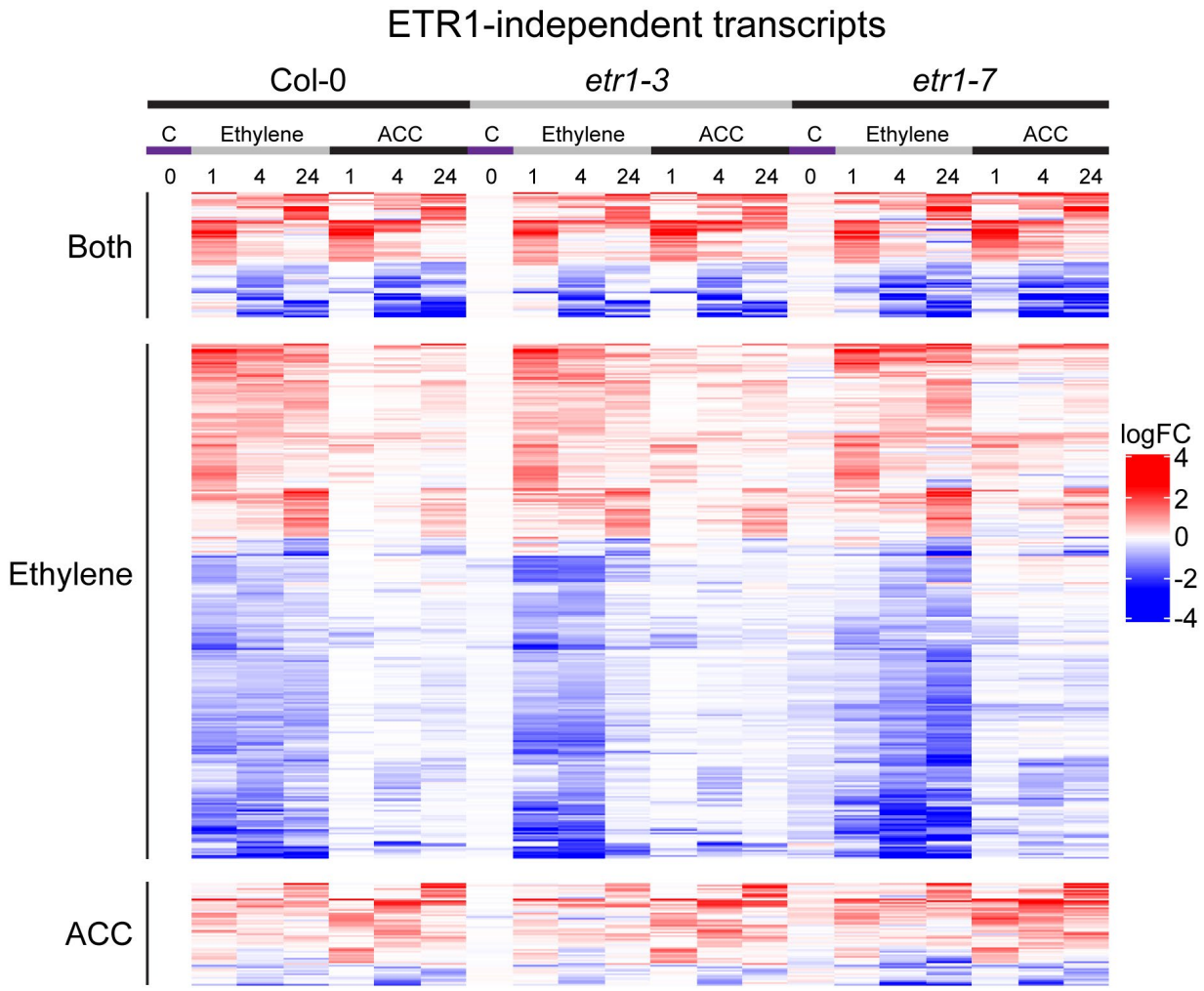

Figure 7. ETR1-independent transcript heatmap revealed genotype and treatment independent changes in transcript abundance. This comparison of transcript abundance across treatments and genotypes revealed a set of genes that responded to ethylene and/or ACC treatment in all genotypes. Genes which respond to ethylene or ACC in all three genotypes were considered receptor-independent (since transcript abundance should have been constant in *etr1-3* and *etr1-7)*. Significant differences were defined as having $|\log_2 FC| > 0.5$ and adjusted p-value < 0.01. Transcripts are divided based on which treatment qualifies as ETR1-independent. $\log_2 FC$ is reported relative to untreated Col-0. Genes are split into three groups based on whether they met our ETR1-independent criteria in ethylene only (488 transcripts), ACC only (95 transcripts), or both treatments (117 transcripts).

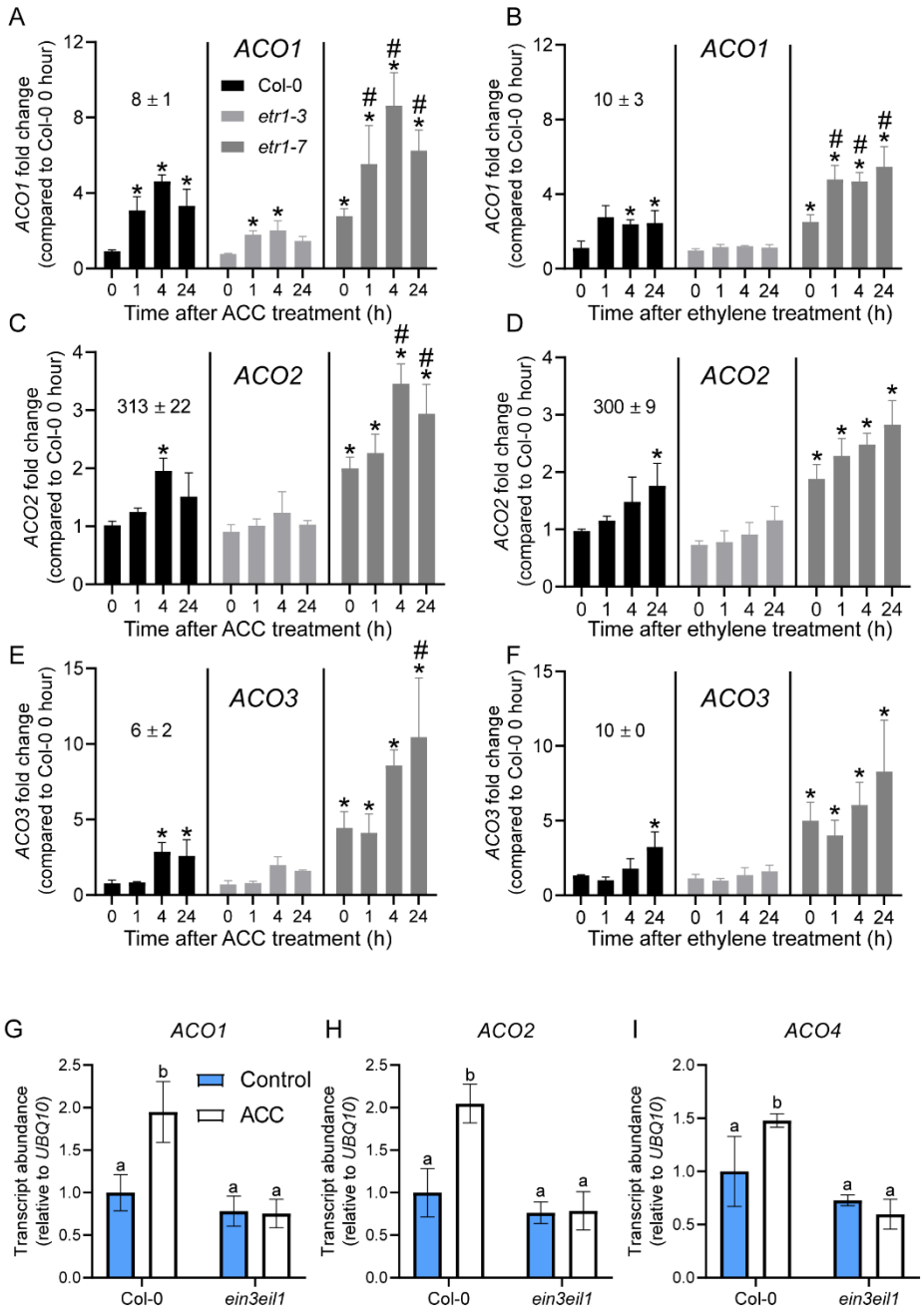

Figure 8. Transcript abundance of ETR1-dependent and/or EIN3/EIL1-regulated *ACO*s. (A-F) Normalized transcript abundance was calculated for *ACO1, ACO2*, and *ACO3* by taking average TPM for each time point and reporting it relative to the average TPM of untreated Col-0. Asterisks indicate statistical significance (p-value < 0.01) compared to Col-0 time 0. Pound symbols indicate statistical significance (p-value < 0.01) compared to *etr1-7* time 0 and are displayed only for *etr1-7*. Error bars represent SD. (G-I) Transcript abundance in Col-0 and *ein3eil1* samples treated with and without 0.75 µM ACC for 4 hours was quantified using RT-qPCR. The average of three biological replicates are reported with error bars representing SD. Statistical significance was defined as p-value < 0.05 using Tukey's multiple comparisons test.

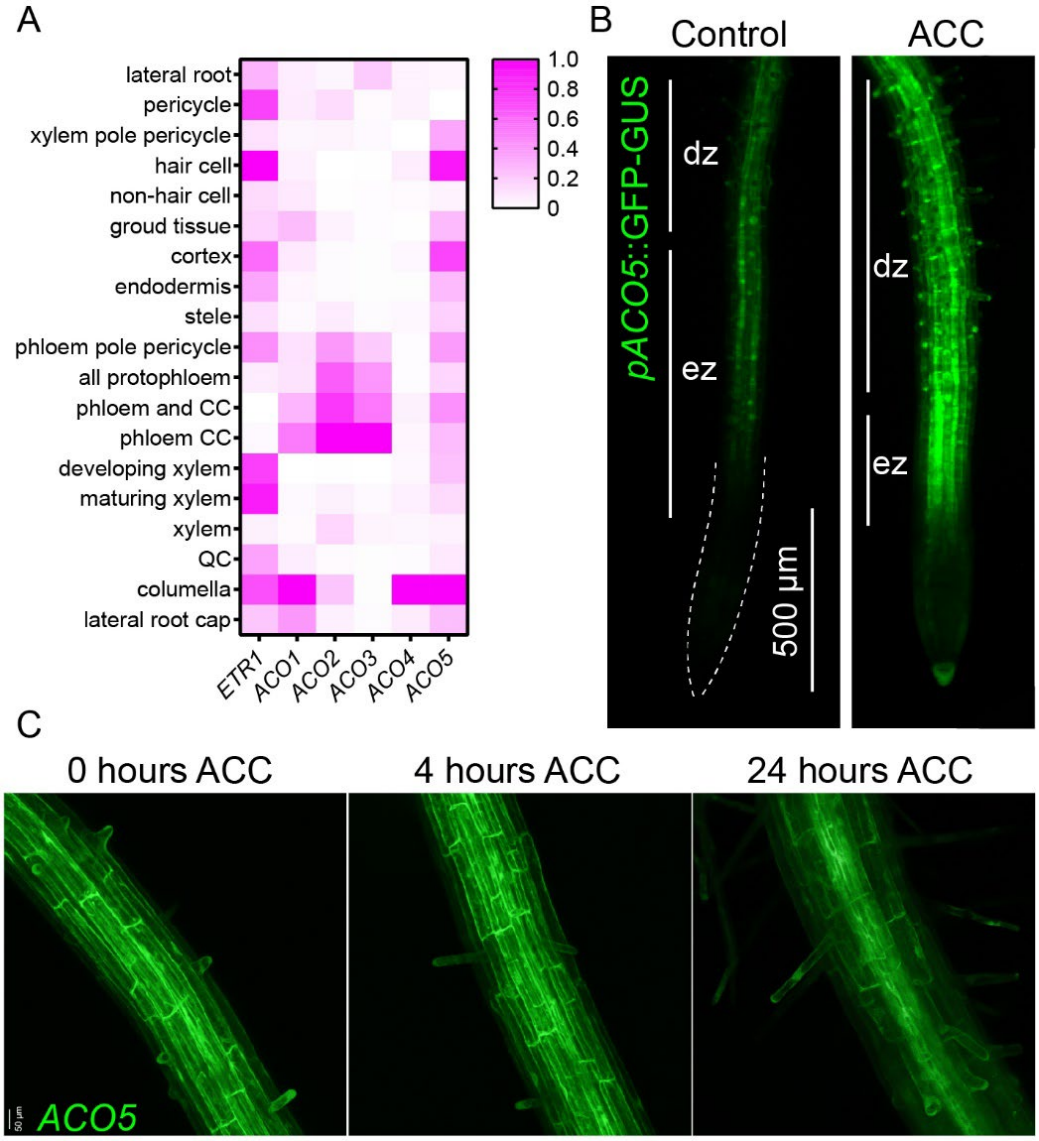

Figure 9. *pACO5*::GFP-GUS is expressed in roots including root hairs. (A) Publicly available root cell type data reported as a heatmap (Brady et al., 2007). Data has been scaled and normalized to the tissue with the highest expression for each transcript. (B) Roots of five-day-old *pACO5*::GFP-GUS seedlings treated with and without 0.75 µM ACC for 4 hours with images captured on a fluorescent stereomicroscope. DZ, differentiation zone. EZ, elongation zone. Scale bar is 500 µm. (C) Roots of 5-day-old *pACO5*::GFP-GUS seedlings treated with 0.75 µM ACC for the indicated time were imaged by laser scanning confocal microscopy. Scale bar = 50 µm.

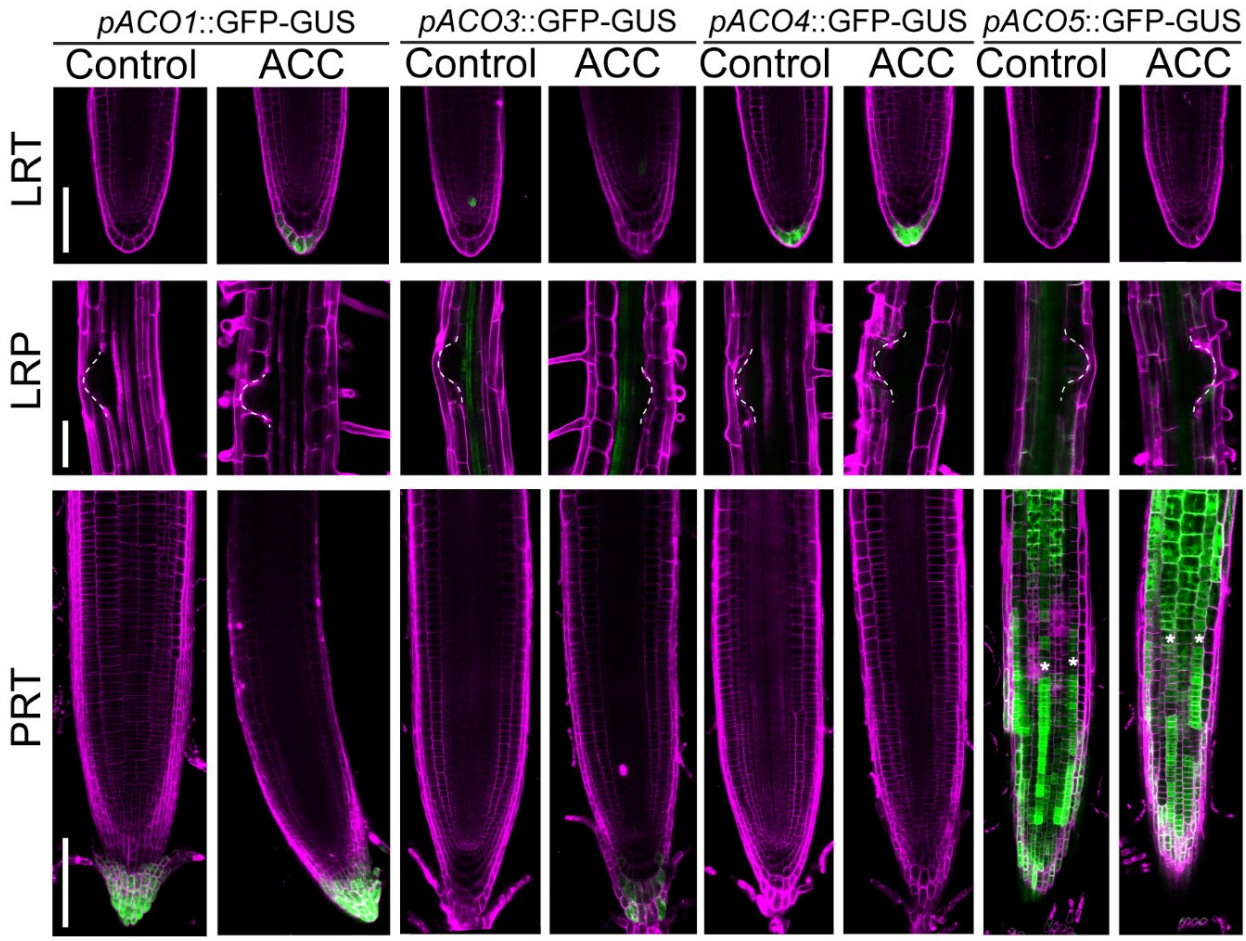

1462

1463 **Figure 10. *ACO* transcripts are synthesized in distinct root tissues in response to ACC**
1464 **treatment.** 10-day-old *pACO*::GFP-GUS seedlings treated with and without 0.75 µM ACC for
1465 five days. Abbreviations for root regions are primary root tip (PRT), lateral root primordium
1466 (LRP), and lateral root tip (LRT). Scale bar is 150 µm for PRT and LRT images and 100 µm for
1467 LRP images.

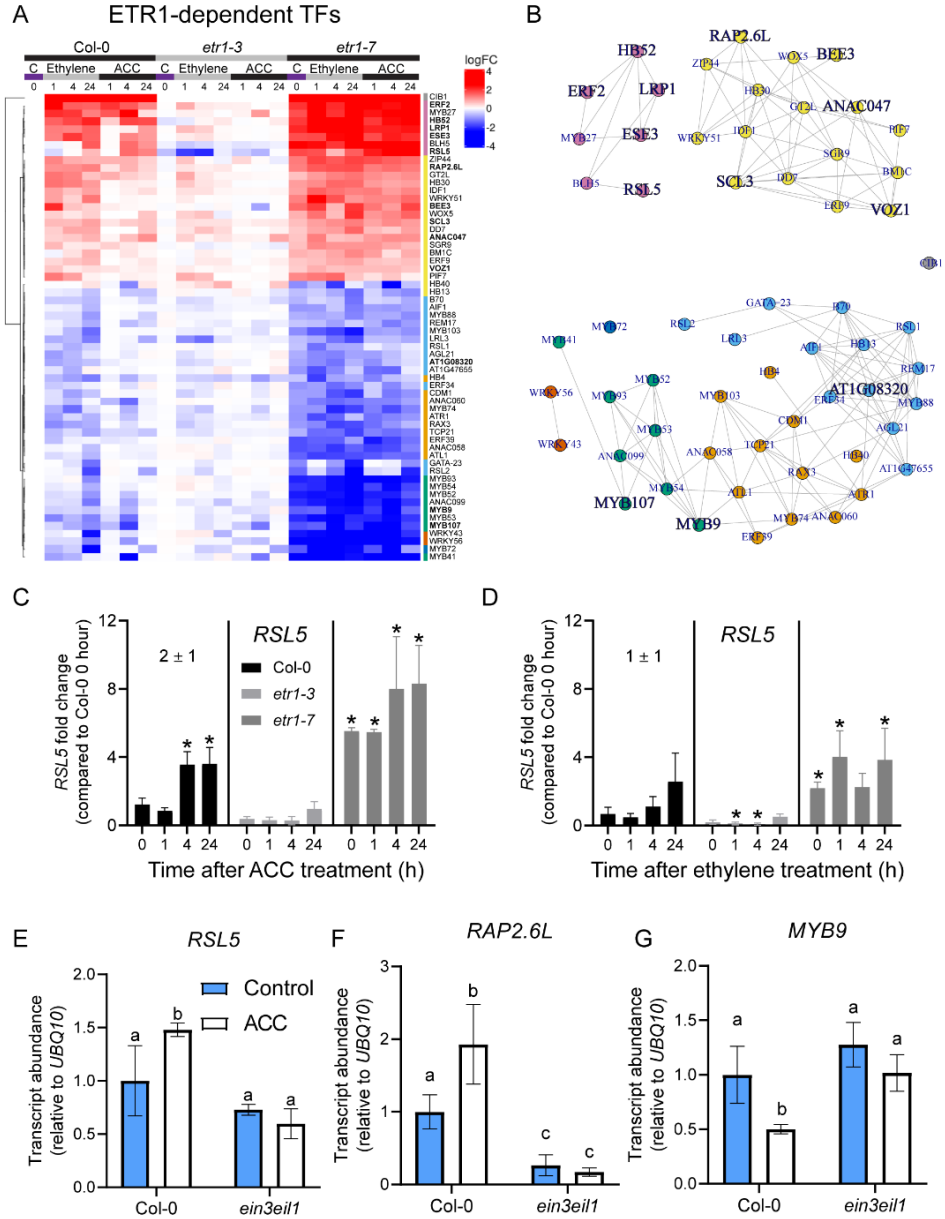

Figure 11. ETR1-dependent transcripts annotated as transcription factors (TFs) exhibit diverse expression patterns. (A) Heatmap of transcript abundance of the 60 ETR1-dependent transcripts that are predicted to encode TFs (reported as log2FC relative to Col-0 time 0). Colors next to gene names correspond to colors in the PaLD network. (B) PaLD network of the ETR1-dependent TFs, with EIN3 direct targets highlighted on the network in large, bold font. The node for CIB1 was positioned more closely to the main network to conserve space. (C, D) RSL5 normalized transcript abundance was calculated by taking average TPM for each time point and reporting it relative to the average TPM of untreated Col-0. (E-G) Transcript abundance in the roots of Col-0 and ein3eil1 seedlings treated with and without 0.75 µM ACC for four hours. Error bars represent SD. Statistical significance was defined as $P < 0.05$ according to Tukey's multiple comparisons test.

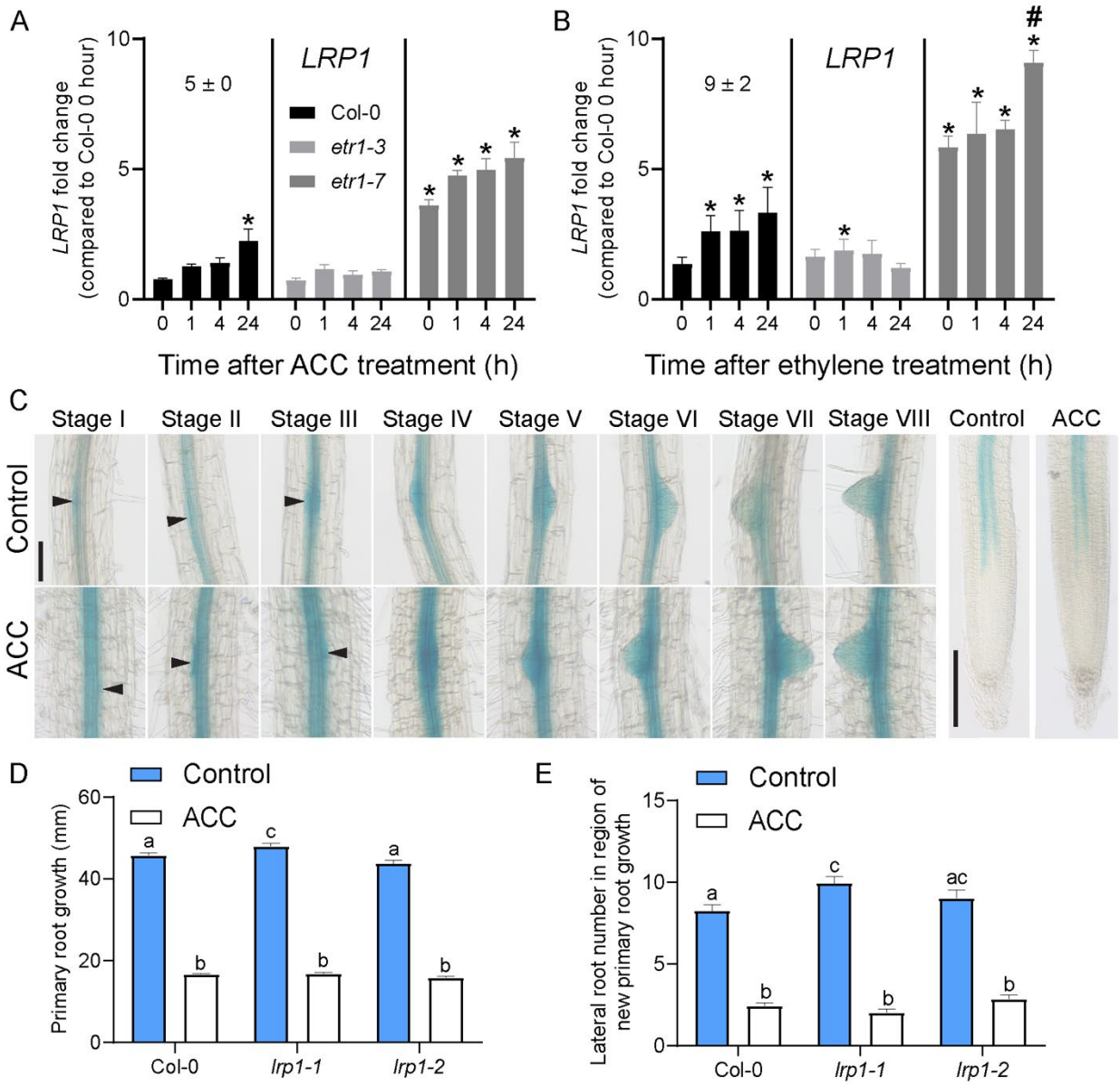

Figure 12. *ProLRP1*::GUS reporter results are consistent with higher LRP1 expression in lateral root primordia in response to ACC treatment. (A, B) *LRP1* normalized transcript abundance was calculated by dividing the TPM of each time point by the average TPM of untreated Col-0. Error bars are SD. (C) Images of lateral root primordia of 10-day-old GUS-stained *proLRP1*::GUS seedlings in the presence and absence of 0.75 µM ACC after five days. Arrows point to stage I-III primordia. Scale bar is 100 µm. Quantification of (D) primary root growth, (E) the number of lateral roots in the region of new root growth in Col-0, *lrp1-1*, and *lrp1-2* in the presence and absence of 0.75 µM ACC after five days. Error bars are SD. Statistical significance is defined as p-value < 0.05 according to Tukey's multiple comparisons test.